the plant journal

SEB SOCIETY FOR EXPERIMENTAL BIOLOGY

The Plant Journal (2024) **120,** 272–288 doi: 10.1111/tpj.16985

AAO2 impairment enhances aldehyde detoxification by AAO3 in Arabidopsis leaves exposed to UV-C or Rose-Bengal

Zhadyrassyn Nurbekova[1,2], Sudhakar Srivastava[1], Zai Du Nja[3], Kusum Khatri[1], Jaykumar Patel[1], Babita Choudhary[1], Veronika Turečková[4], Miroslav Strnad[4], Edyta Zdunek-Zastocka[5], Rustem Omarov[2], Dominic Standing[6] and Moshe Sagi[6,7,8,*]

[1]*Jacob Blaustein Center for Scientific Cooperation, The Jacob Blaustein Institutes for Desert Research, Ben-Gurion University of the Negev, Sede Boqer Campus, Beer Sheva 8499000, Israel,*

[2]*Department of Biotechnology and Microbiology, L.N. Gumilyov Eurasian National University, Astana, Kazakhstan,*

[3]*The Albert Katz International School for Desert Studies, The Jacob Blaustein Institutes for Desert Research, Ben-Gurion University of the Negev, Sede Boqer Campus, Beer Sheva 8499000, Israel,*

[4]*Laboratory of Growth Regulators, The Czech Academy of Sciences, Institute of Experimental Botany, Palacky University, Slechtitelu 27, Olomouc CZ-78371, Czech Republic,*

[5]*Department of Biochemistry and Microbiology, Warsaw University of Life Sciences – SGGW, Nowoursynowska 159, Warsaw 02-776, Poland,*

[6]*The Albert Katz Department of Dryland Biotechnologies, French Associates Institute for Agriculture and Biotechnology of Dryland, The Jacob Blaustein Institutes for Desert Research, Ben-Gurion University of the Negev, Sede Boqer Campus, Beer Sheva 8499000, Israel,*

[7]*Katif Research Center, Sedot Negev, Israel, and*

[8]*Ministry of Science and Technology, Netivot, Israel*

Received 9 May 2024; revised 20 July 2024; accepted 31 July 2024; published online 27 August 2024.
*For correspondence (e-mail gizi@bgu.ac.il)
[Correction added on 2 May 2025 after first online publication: In the author byline, the names of Veronika Turečková and Miroslav Strnad are misspelled and it has been corrected in this version.]

SUMMARY

Among the three active aldehyde oxidases in *Arabidopsis thaliana* leaves (AAO1-3), AAO3, which catalyzes the oxidation of abscisic-aldehyde to abscisic-acid, was shown recently to function as a reactive aldehyde detoxifier. Notably, *aao2KO* mutants exhibited less senescence symptoms and lower aldehyde accumulation, such as acrolein, benzaldehyde, and 4-hydroxyl-2-nonenal (HNE) than in wild-type leaves exposed to UV-C or Rose-Bengal. The effect of *AAO2* expression absence on aldehyde detoxification by AAO3 and/or AAO1 was studied by comparing the response of wild-type plants to the response of single-functioning *aao1* mutant (*aao1S*), *aao2KO* mutants, and single-functioning *aao3* mutants (*aao3Ss*). Notably, *aao3Ss* exhibited similar aldehyde accumulation and chlorophyll content to *aao2KO* treated with UV-C or Rose-Bengal. In contrast, wild-type and *aao1S* exhibited higher aldehyde accumulation that resulted in lower remaining chlorophyll than in aao*2KO* leaves, indicating that the absence of active AAO2 enhanced AAO3 detoxification activity in *aao2KO* mutants. In support of this notion, employing abscisic-aldehyde as a specific substrate marker for AAO3 activity revealed enhanced AAO3 activity in *aao2KO* and *aao3Ss* leaves compared to wild-type treated with UV-C or Rose-Bengal. The similar abscisic-acid level accumulated in leaves of unstressed or stressed genotypes indicates that aldehyde detoxification by AAO3 is the cause for better stress resistance in *aao2KO* mutants. Employing the sulfuration process (known to activate aldehyde oxidases) in wild-type, *aao2KO*, and *molybdenum-cofactor sulfurase* (*aba3-1*) mutant plants revealed that the active AAO2 in WT employs sulfuration processes essential for AAO3 activity level, resulting in the lower AAO3 activity in WT than AAO3 activity in *aao2KO.*

Keywords: Arabidopsis, aldehyde oxidase, reactive aldehydes, senescence, UV-C irradiation, Rose-Bengal, aldehyde toxicity, sulfuration.

INTRODUCTION

Aldehyde oxidase (AO) is a cytoplasmic multicomponent domain enzyme which contains FAD, Fe-S, and molybdenum cofactor (MoCo) as its prosthetic groups and thus belongs to the family of Mo-hydroxylases (Koshiba et al., 1996; Yesbergenova et al., 2005). AO catalyzes the

oxidation of a variety of aldehydes and heterocyclic compounds, thereby converting them to the respective carboxylic acids (Akaba et al., 1998; Koshiba et al., 1996; Seo, Koiwai, et al., 2000; Seo & Koshiba, 2002; Srivastava et al., 2017). AO enzymes have a relatively broad substrate specificity and their role in response to environmental stress factors was previously reported (Omarov et al., 1998; Sagi et al., 1998; Yergaliyev et al., 2016; Zdunek-Zastocka et al., 2004; Zdunek-Zastocka & Sobczak, 2013). Early observations demonstrated the presence of four *AO* genes in *Arabidopsis thaliana* and their organ localization as well as their expression dependency on the developmental stage of the organ. *Arabidopsis* AO1 (AAO1) was shown to be mainly expressed in seeds, roots, and seedlings, AAO2 in seedlings and roots, AAO3 in rosettes, seeds, and roots, whereas AAO4 is mainly expressed in siliques (González-Guzmán et al., 2004; Koiwai et al., 2004; Seo, Koiwai, et al., 2000; Srivastava et al., 2017). Additionally, it was shown that AAO1 is involved in the oxidation of indole-3-carbaldehyde (ICHO) to indole-3-carboxylic acid (ICOOH) (Bottcher et al., 2014), and AAO4 is involved in benzoic acid biosynthesis (Ibdah et al., 2009). It was also demonstrated that AAO4 can efficiently oxidize toxic aldehydes and thus delay silique senescence (Srivastava et al., 2017). Recently it was shown that AAO3 known to oxidize abscisic aldehyde (ABal) to abscisic acid (ABA) (Seo, Koiwai, et al., 2000; Seo, Peeters, et al., 2000) can protect rosette leaves from stress-induced aldehyde toxicity (Nurbekova et al., 2021). Additional roles for AAO2 and the other AAOs require further investigation.

Plants are constantly exposed to environmental factors such as extreme temperature, drought, salinity, pathogen attack, and natural aging which leads to enhanced generation of aldehydes, downstream to reactive oxygen species (ROS) production. Above a certain level, specific to each of the aldehydes, the elevated level of aldehydes can be toxic, leading to the oxidative injury of plants, enhanced chlorophyll degradation, hastened senescence, and even cell death (Biswas & Mano, 2016; Nurbekova et al., 2021; Srivastava et al., 2017). Detoxification of the increased aldehydes is therefore essential for plant survival and was shown by aldehyde dehydrogenases [ALDH; EC 1.2.1.3 (Stiti et al., 2011; Sunkar et al., 2003; Widhalm & Dudareva, 2015)], aldo-keto reductases (AKR; EC 1.1.1.2), aldehyde reductases [ALR; EC 1.1.1.2 (Oberschall et al., 2000; Yamauchi et al., 2011)], 2-alkenal reductases [AER, EC 1.3.1.74 (Mano et al., 2002)], glutathione transferase tau isozymes [GST (Mano et al., 2019)], and aldehyde oxidases 3 and 4 (Nurbekova et al., 2021; Srivastava et al., 2017).

Recently we observed in Arabidopsis rosette leaves a significant reduction of AAO2 in-gel activity in plants exposed to UV-C irradiation (Nurbekova et al., 2021, figure 7j), which led us to investigate a possible role of AAO2 in plants exposed to abiotic stresses. The current study showed significantly greater detoxification of aldehydes in the aldehyde oxidase 2 knock-out (*aao2KO*) mutants than in WT in response to UV-C irradiation or Rose-Bengal application. The application of such stresses resulted in higher chlorophyll degradation in WT leaves relative to the *aao2KO* mutant. Since *aao2KO* mutant leaves contain active AAO1 and AAO3, one or both enzymes could be responsible for better aldehyde detoxification. By using RNA interference (RNAi) on the various T-DNA KO mutants impaired in one of the three aldehyde oxidases (AAO1-3), *aao1S* and *aao3S* single-functioning mutants were generated and were exposed to UV-C irradiation or Rose-Bengal application. Notably, independent *aao3* single-functioning mutants (*aao3Ss*) containing fully active AAO3 exhibited lower aldehyde accumulation as compared to WT, while *aao1* single (*aao1S*) mutant, containing fully active AAO1 resulted in similar or higher level of aldehyde accumulation as well as higher chlorophyll degradation as compared to WT under UV-C irradiation or Rose-Bengal application, indicating that the impairment of AAO2 causes the enhancement of AAO3 activity and the capacity of carbonyl aldehyde detoxification in Arabidopsis.

RESULTS

Protein expression analysis of *aao2KO* and identification of AAO2 activity

To investigate the possible roles of AAO2 in aldehyde detoxification, two independent knock-out (KO) lines of *aao2* mutants [SALK_104895 (KO-95) and SAIL_563_G09 (KO-563)] each carrying exon inserted T-DNA were employed. The homozygosity of the two *aao2KO* lines was examined. The absence of amplicon when using gene-specific left and right primers (LP + RP) and the presence of amplicon with RP and T-DNA specific primers (LB1.3/LB2) indicated the homozygous lines for the knockout mutants of *AAO2* (Figure 1A; Table S1). The transcript expression of *AAO2* was determined by quantitative polymerase chain reaction (qPCR) using gene-specific primers from either side of T-DNA insertion (Table S2A). No expression was detected in *aao2KO* mutants, whereas in WT the expression of *AAO2* was evident (Figure 1B) and the amplicons were verified by sequencing (Table S2B). Crude protein extracts from WT rosette leaves and both *aao2KOs* were employed for the determination of AAO2 in-gel activity by using *trans*-2-hexanal as a substrate (Nurbekova et al., 2021). The oxidation of *trans*-2-hexanal led to a highest intensity in the most migrated band and a weaker intensity in the middle band in WT, whereas the absence of the middle and the most migrated activity bands was evident in both *aao2KOs*. Notably, the only upper activity band that appeared in *aao2KOs* had a higher band intensity compared to WT (Figure 1C). To further verify that among the aldehyde oxidases only AAO2 generates the most migrated (lowest) activity band, the lowest activity band in *aao1*, *aao3* KOs, and WT (Figure 1C) was

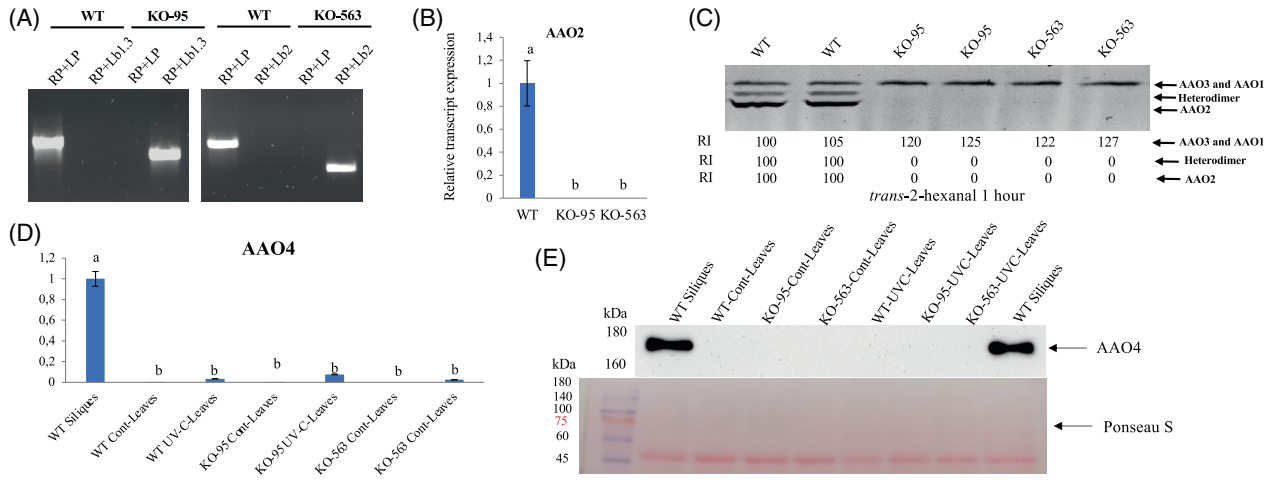

Figure 1. Characterization of *Arabidopsis* aldehyde oxidase 2 mutants.
(A) Verification of AAO2 knockout mutants {*aao2* [SALK_104895 (KO-95) and SAIL_563_G09 (KO-563)]} by PCR using the combination of gene-specific primers (LP and RP) and specific primer flanking T-DNA insertion stretches (LB 1.3 or LB2, respectively).
(B) Relative transcript expression of *AAO2* (At3g43600) in wild-type (WT) and the two *aao2* mutants' rosette leaves. The expression of the *AAO2* in each genotype was compared against *AAO2* in WT after normalization to *Arabidopsis EF-1a* (At5g60390) as the housekeeping gene product and presented as the relative expression. Values means ± SE (n = 3).
(C) *Arabidopsis* aldehyde oxidases (AAOs) in-gel activity in WT and *aao2* (KO-95 and KO-563). One hundred microgram protein extract from 3-week-old plants' rosette leaves were fractionated by NATIVE PAGE and AO activity detection with 1 mM *trans*-2-hexanal as the substrate was determined in a reaction solution containing 100 mM Tris-HCl (pH 7.5), 1 mM 3-(4,5-dimethylthiazol-2-yl)-2,5-diphenyltetrazolium bromide and 0.1 mM phenazine methosulfate. The arrow indicates the position of the activity bands generated by AAO1 and AAO3 proteins (uppermost band), middle (heterodimer containing AAO2 with AAO1 and/or with AAO3), and AAO2 (lowermost band) 1 h after substrate insertion into the reaction solution.
(D) Relative transcript expression of *AAO4* (AT1G04580) in 7–9 days post anthesis WT siliques, as positive control, was compared to *AAO4* expression in rosette leaves in control and UV-C (250 mJ) treated WT and *aao2* (KO-95 and KO563) plants. The expressions were compared after normalization to *Arabidopsis EF-1a* as the housekeeping gene product and presented as the relative expression. Values means ± SE (n = 3). Differences in transcript expressions [in (B) and (D)] were compared among all the genotypes, and different letters show the significant difference between genotypes (Tukey's honest significant difference, HSD, P value <0.05).
(E) Immunoblot analysis of AAO4 in WT siliques compared to AAO4 protein expression in rosette leaves of control and UV-C (250 mJ) treated WT and aao2 (KO-95 and KO563) plants. Twenty five microgram crude protein extract loaded in each lane was separated by using SDS-PAGE, transferred to polyvinylidene difluoride membranes and were detected by using specific AAO4 antibody as employed by us before (Srivastava et al., 2017). Relative intensity (RI) of the activity bands was estimated by using ImageJ software (https://imagej.nih.gov/ij/). Each of the obtained band intensities was compared with that obtained with WT (employed as 100%) and presented as relative intensity (RI). Western blot results repeated using two independent biological experiments and one representative is presented. The precision of proteins identified by AAO4-specific antibody, and proteins stained by Ponseau S is presented by Protein Standards (Bio-Rad).

excised and peptide sequencing was carried out. The sequencing of trypsinized peptides of the lowest activity band of WT, *aao1*, and *aao3* KO mutants revealed 8, 6, and 8 unique peptides of AAO2, respectively (Table S3). Additionally, AVSGNLCR and IPTVDTIPK were identified in AAO2 activity band of WT, which share identical sequences in AAO1 and AAO3, respectively. VGGGFGGK peptide of AAO2 that was identified in AAO2 activity band in *aao1KO* shares identical sequences in AAO1 and AAO3. Similarly, the ASGEPPLLLAASVHCATR peptide of AAO2 identified in *aao3* shares an identical sequence with AAO3.

Notably, similar to the identification of the least migrated activity band as AAO1 and AAO3 proteins [with specific peptide identification and the absence of AAO2 and AAO4 unique peptides, as shown in Nurbekova et al. (2021), table S3], the most migrated activity band also lacks AAO4 unique peptides. Therefore, it is highly likely that this band belongs to the AAO2 protein activity band (see Table S3).

Although no AAO4 activity or protein expression was detectable in WT rosette leaves after harsh drought stress (Srivastava et al., 2017, figure S4D), we examined the expression of AAO4 transcript and protein in *aao2KO* mutants under further stress conditions. Interestingly, examination of the AAO4 transcript expression by specific primers (Table S2A), as done previously (Srivastava et al., 2017), revealed that the transcript expressions in rosette leaves of WT and both aao2 KO mutants exposed to control or UV-C stress (250 mJ) conditions were less than 8% of the expression in unstressed 7–9 days post anthesis WT siliques used as positive control (Figure 1D). Accordingly, immunoblot analysis using an AAO4-specific antibody (Srivastava et al., 2017) revealed the absence of protein expression in the stressed and unstressed rosette leaves of WT and both aao2 KO mutants, whereas a significant AAO4 protein expression was seen in WT siliques (Figure 1E), indicating that any residual effect of AAO4 in rosette leaves can be ignored.

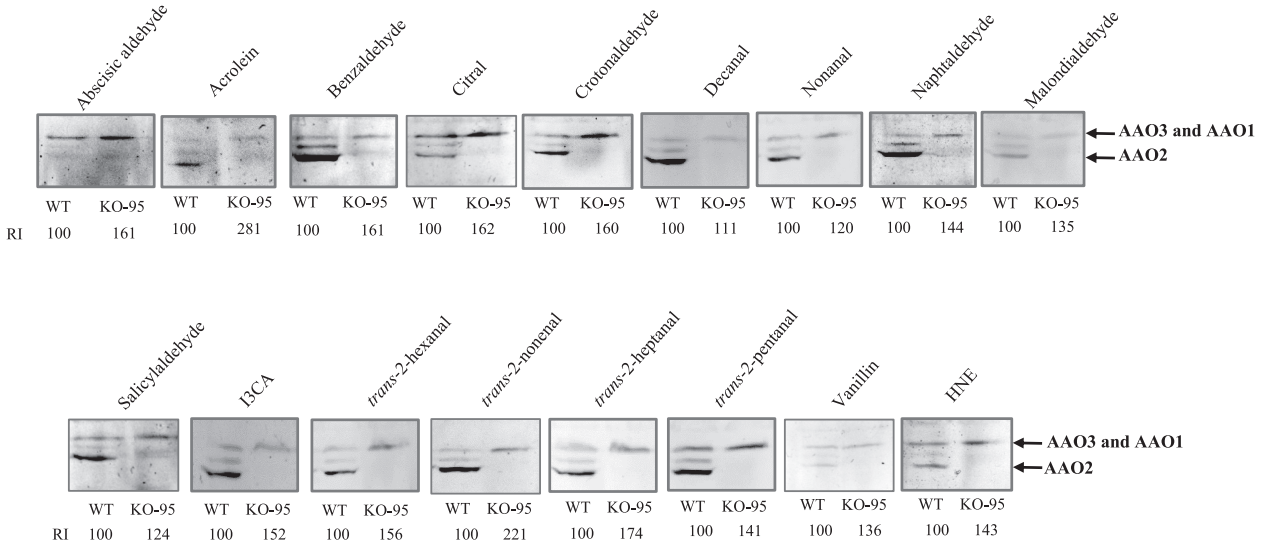

Figure 2. *Arabidopsis* aldehyde oxidases (AAOs) activity assessment in WT and *aao2* [SALK104895 (KO-95)] mutant using different aldehydes as the substrate. One hundred microgram protein extracted from rosette leaves of 23-day-old WT and KO-95 mutant plants were fractionated by NATIVE PAGE and AO activity with indicated aldehyde as the substrate was carried out. AO enzyme activity was determined in a reaction solution containing 100 mM Tris-HCl (pH 7.5), 1 mM 3-(4,5-dimethylthiazol-2-yl)-2,5-diphenyltetrazolium bromide, 0.1 mM phenazine methosulfate, and 1 mM aldehydes, except for HNE and abscisic aldehyde that were applied with 0.25 and 0.1 mM, respectively. The reaction was stopped after 3 h and after 2 h for abscisic aldehyde, by immersing the gel in 5% acetic acid solution. Thereafter gel images were captured and analyzed for relative intensity (RI) using ImageJ software (http://imagej.nih.gov/ij/) for the slowest (uppermost) migrated band intensity compared to the WT uppermost migrated band as reference (100%).

Mutation in AAO2 confers higher capacity of oxidizing aldehydes in *aao2KO* mutants as compared to WT

The capacity of *aao2* mutant to oxidize a range of aldehydes including reactive aldehydes was compared to WT to get more insight into the function of AAO2. The crude protein extracted from the rosette leaves of *aao2KO* (KO-95) and WT was fractionated by NATIVE PAGE. Significantly, knockout of *aao2KO* (KO-95) mutant exhibited only the upper activity band, whereas WT exhibited additional middle and the lowest activity bands (Figures 1C and 2). The application of various aldehydes at the level of 1 mM [except for 4-hydroxyl-2-nonenal (HNE) (0.25 mM) and ABal (0.1 mM)] exhibited that upper in-gel activity band generated by *aao2* (*KO-95*) extracted proteins had a more intense activity band (higher activity level) with almost all aldehydes employed as substrates as compared with WT. These results indicate that the absence of AAO2 enhances the oxidation capacity of aldehydes by AAO3 and/or AAO1 (Figure 2), suggesting a role for AAO2 in the homeostasis of aldehydes level by modulating another/other aldehyde oxidase/s activity in plant leaves.

UV-C irradiation results in a faster aldehyde-induced senescence in WT compared to *aao2* mutants

The generation of toxic aldehydes which leads to plant senescence is a major response of plants exposed to abiotic stresses. Among the abiotic stresses, UV-C was shown recently to induce premature senescence of siliques and rosette leaves in *Arabidopsis* by enhancing the generation of toxic aldehydes (Nurbekova et al., 2021; Srivastava et al., 2017). Thus, it was reasonable to study how UV-C irradiation will affect *aao2KO* mutant in the absence of AAO2. Notably, the application of 250 mJ of UV-C irradiation resulted in earlier senescence and more significant chlorophyll loss in WT leaves as compared to the two *aao2KOs* (*KO-95* and *KO-563*) mutants 3 days after the application of the UV-C irradiation (Figure 3A,B). Accordingly, Western blot analyses of the rosette leaves crude protein extracts revealed that UV-C irradiation caused a higher degradation level of chloroplast localized proteins in WT than in *aao2KOs*, such as the large subunit of Rubisco, the most abundant protein in green tissue (Bindschedler & Cramer, 2011), and D1 protein, a component of the reaction center of PSII (Keren et al., 1997), exhibiting a clear hallmark of more senescent leaves in WT compared to *aao2KOs* (Figure S1A,B).

Determination of the aldehyde level in UV-C treated plants revealed significantly higher levels of acrolein, benzaldehyde, and HNE in WT than in the leaves of *aao2KO* mutant (Figure 3C; Figures S2 and S3). An in-gel assay that was carried out to examine the AAO3 and AAO1 activity levels in control (UV-C untreated) and in UV-C treated WT, *aao2KO*, *aao3KO* (containing active AAO1 and AAO2) and *aao1KO* (containing active AAO3 and AAO2) mutants. Using *trans*-2-nonenal or benzaldehyde as the substrates revealed enhanced intensity in the most upper (least migrated) activity band in *aao2* mutant compared to WT,

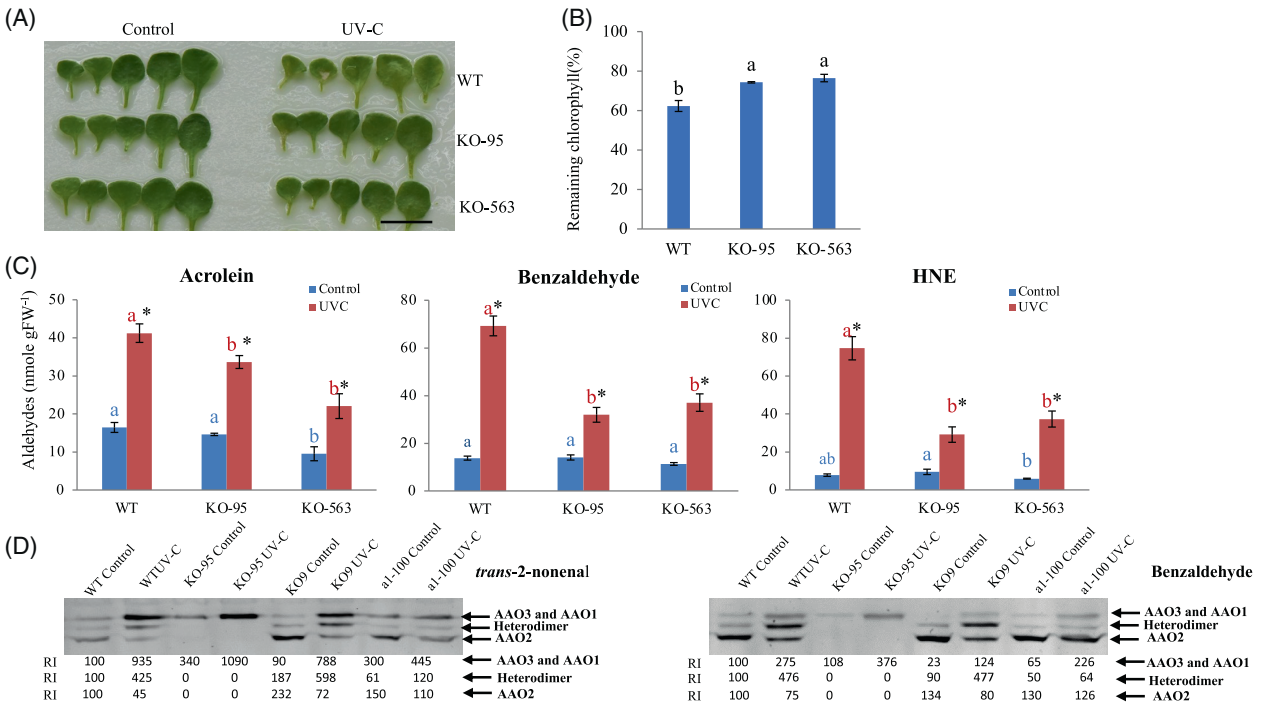

Figure 3. Determination of UV-C-irradiation-induced senescence and senescence-related factors in rosette leaves of *Arabidopsis* wild-type (WT) and *aao2KO* [SALK_104895 (KO-95) and SAIL_563_G09 (KO-563)] mutant plants.

(A) Representative photograph of WT and *aao2* rosette leaves in response to UV-C irradiation. Twenty-one-day post-germination plants exposed to 250 mJ of UV-C irradiation were kept in a growth room for 72 h and thereafter documented. Scale bar = 1 cm. Rosette leaves were collected 3 days after UV-C treatment, and rosette leaves of plants that were not exposed to UV-C were used as the control. First five leaves, oldest to youngest, from left to right are presented.

(B) Remaining chlorophyll in leaves after UV-C treatment.

(C) Indicated aldehyde profiling in control (blue bars) and UV-C treated (red bars) plants. Leaves from three different plants were taken as one replica, and the bars show the average of at least four replicas. Different letters above the bar indicate significant differences (Tukey–Kramer HSD test, $P < 0.05$). Asterisk shows significant differences between treatments within the same genotype (Student's *t* test, $P < 0.05$).

(D) Aldehyde oxidases (AAOs) in gel activity in control and UV-C treated WT, *aao2* (KO-95), *aao3* [SAIL_78_H09 (KO9)], and *aao1* [SALK_018100 (a1-100)]. 150 μg crude protein extracted from rosette leaves were fractionated by NATIVE PAGE and were used for the in-gel activity, assayed for 1 h in solution containing 100 mM Tris-HCl (pH 7.5), 1 mM 3-(4,5-dimethylthiazol-2-yl)-2,5-diphenyltetrazolium bromide, 0.1 mM phenazine methosulfate, and 1 mM *trans*-2-nonenal or benzaldehyde as the aldehyde substrate. The gels were scanned, and the intensity of the activity bands was estimated using ImageJ software (http://imagej.nih.gov/ij/) and compared with the intensity obtained with UV-C untreated (control) WT (employed as 100%) and presented as relative intensity (RI).

aao1KO, and *aao3KO*, both under control and UV-C stress conditions, indicating that the absence of active AAO2 enhances the activity of AAO1 and AAO3. Examination of AAO1 in *aao3* and AAO3 activity in *aao1* mutant revealed that both enzyme activities were enhanced with both aldehyde substrates used, as the result of UV-C irradiation (Figure 3D). Parallel to AAO1 and AAO3 increase, the heterodimer's activity bands [middle bands (Akaba et al., 1999; Koiwai et al., 2004)] in WT (AAO1:AAO2 + AAO3:AAO2) and *aao3* mutant (AAO1:AAO2) exhibited higher increase in response to the applied stress than the heterodimer activity in *aao1* mutant (AAO3:AAO2) with either aldehyde substrate used (Figure 3D). Notably, the AAO3 and/or AAO1 enhanced activity in plants exposed to UV-C irradiation was followed by AAO2 activity (most migrated band) decrease in WT, *aao1KO*, and *aao3KO* plants. In contrast, the absence of AAO2 in *aao2KO* plants resulted in higher AAO3 and/or AAO1 activity compared to WT plants, resulting in a higher level of remaining chlorophyll and chloroplast localized proteins, the result of better aldehydes detoxification capacity compared to WT (Figure 3A–D).

Application of Rose-Bengal confers aldehyde-induced earlier senescence in WT compared to *aao2* mutant leaves

Applying 0.05 mM Rose-Bengal by spray, as another abiotic stress type, induced early senescence symptoms in rosette leaves of WT 3 days after treatment, whereas *aao2* leaves showed much less visible senescence symptoms (Figure 4A). Detection of the remaining chlorophyll revealed a significant chlorophyll degradation in leaves of WT 3 days after Rose-Bengal application, whereas the chlorophyll was less degraded in *aao2* leaves (Figure 4B). Accordingly, Western blot analyses of rosette leave crude proteins revealed that similar to UV-C irradiation, Rose-Bengal spray caused an enhanced degradation level of the chloroplast localized large subunit of Rubisco, and D1 proteins, exhibiting a clear hallmark of more senescent

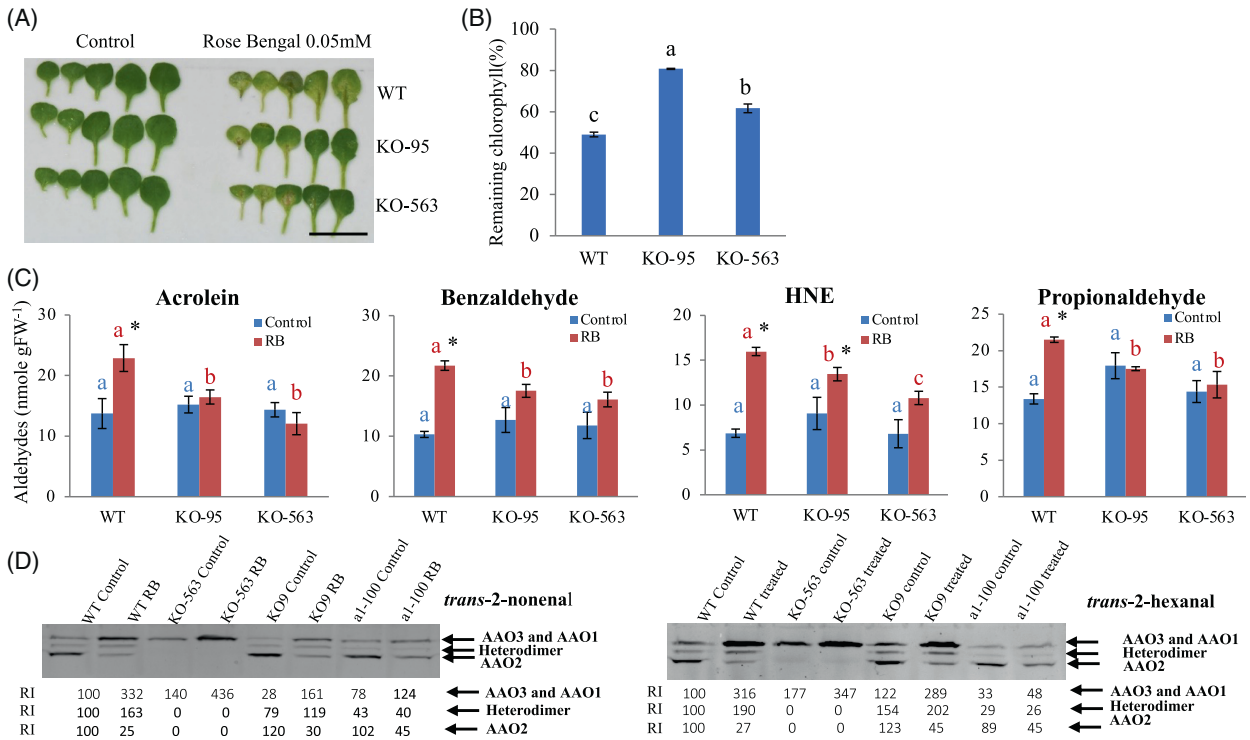

Figure 4. Determination of Rose-Bengal-induced senescence and senescence-related factors in rosette leaves of *Arabidopsis* wild-type (WT) and *aao2KO* [SALK_104895 (KO-95) and SAIL_563_G09 (KO-563)] mutant plants.

(A) Representative photograph of WT and *aao2* rosette leaves in response to Rose-Bengal application. Twenty-three days post germination plants treated with 0.05 mM Rose-Bengal were kept in a growth room for 72 h and thereafter documented. Scale bar = 2 cm. First five leaves, oldest to youngest, from left to right are presented. The rosette leaves were collected 17 h after Rose-Bengal treatment, and rosette leaves of plants that were not exposed to Rose-Bengal were used as the control.

(B) Remaining chlorophyll in first five leaves after Rose-Bengal treatment.

(C) Indicated aldehyde profiling in control (blue bars) and Rose-Bengal treated (red bars) plants. Leaves from three different plants were taken as one replica, and the bars show the average of at least four replicas. Different letters above the bar indicate significant differences (Tukey–Kramer HSD test, $P < 0.05$). Asterisk shows significant differences between treatments within the same genotype (Student's *t* test, $P < 0.05$).

(D) Aldehyde oxidases (AAOs) in gel activity in control and Rose-Bengal treated WT, *aao2* (KO-95), *aao3* [SAIL_78_H09 (KO9)], and *aao1* [SALK_018100 (a1-100)]. 150 μg crude protein extracted from rosette leaves was fractionated by NATIVE PAGE and was used for the in-gel activity, assayed for 1 h in solution containing 100 mM Tris-HCl (pH 7.5), 1 mM 3-(4,5-dimethylthiazol-2-yl)-2,5-diphenyltetrazolium bromide, 0.1 mM phenazine methosulfate, and 1 mM *trans*-2-nonenal or *trans*-2-hexanal as the aldehyde substrate. The gels were scanned, and the intensity of the activity bands was estimated using ImageJ software (http://imagej.nih.gov/ij/) and compared with the intensity of the activity band obtained with Rose-Bengal untreated (control) WT (employed as 100%) and presented as relative intensity (RI).

leaves in WT compared to *aao2KOs* mutants' leaves (Figure S4A,B). Detection of aldehydes 17 h after Rose-Bengal application revealed higher enhancement of acrolein, benzaldehyde, propionaldehyde, and HNE in WT than in the leaves of the 2 *aao2* mutants (Figure 4C; Figures S5 and S6). In-gel AAO activity assay carried out to examine the AAO3 and AAO1 activity levels in the control treated WT and *aao2* mutant using *trans*-2-nonenal or *trans*-2-hexanal as the substrate revealed higher intensity in the most upper activity band in *aao2* mutant compared to WT (Figure 4D). Using *trans*-2-nonenal as the substrate revealed higher AAO3 activity than AAO1 under control conditions, as indicated by the higher intensity in the most upper band in *aao1* compared to *aao3* mutant. In contrast, *trans*-2-hexanal was a preferable substrate for AAO1 activity, as indicated by the higher intensity of the most upper band in *aao3* compared to *aao1* mutant. The application of Rose-Bengal resulted in the enhancement of the uppermost band in WT and all examined mutants, indicating the activation of AAO1 and/or AAO3 in the absence and presence of AAO2 activity. Examination of AAO1 in *aao3* and AAO3 activity in *aao1* mutant exposed to Rose-Bengal revealed that both enzyme activities were enhanced with either aldehyde substrate used (Figure 4D). Interestingly, the heterodimer activity bands in WT (AAO1:AAO2 and AAO3:AAO2) and in *aao3* mutant (AAO1:AAO2) exhibited an increase in response to the applied stress, whereas the heterodimer activity in *aao1* mutant (AAO3:AAO2) tended to show the absence of enhanced intensity with either aldehyde substrate used (Figure 4D). Notably, similar to the UV-C treatment (Figure 3D), the AAO3 and/or AAO1 enhanced activity in plants exposed to Rose-Bengal spray

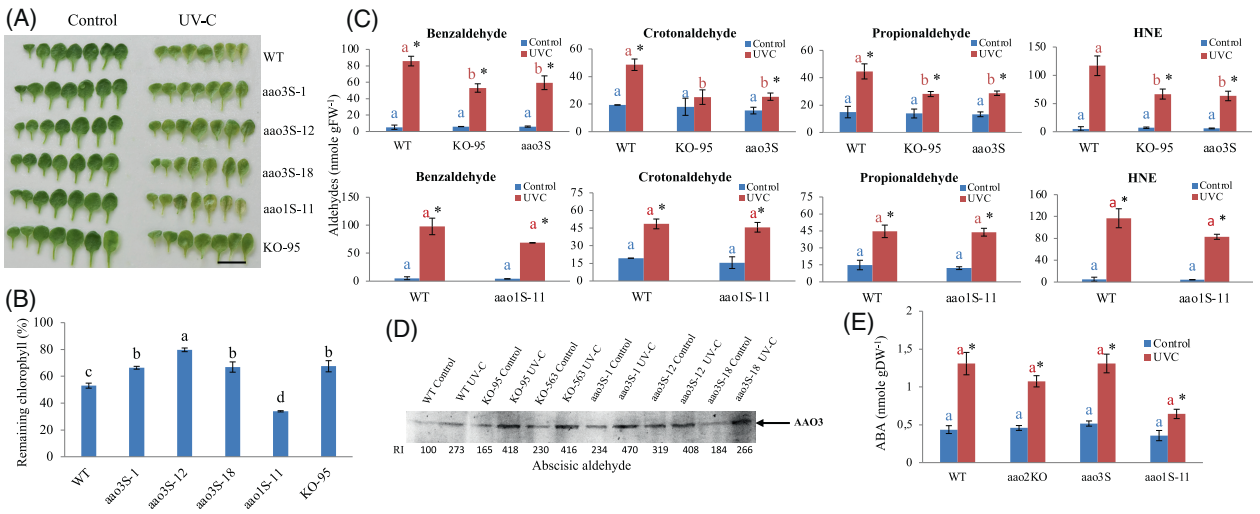

Figure 5. Determination of UV-C-irradiation-induced senescence and senescence-related factors in rosette leaves of *Arabidopsis* aldehyde oxidases single mutants [*aao1Single* (*aao1S*) and *aao3Singles* (*aao3Ss*)], *aao2KO* [SALK_104895 (KO-95)], and wild-type (WT) plants.
(A) Representative photograph of WT, *aao2*, *aao1S*, and *aao3Ss* (*aao3S-1*, *aao3S-12*, *aao3S-18*) rosette leaves in untreated (control) and UV-C irradiation treated plants. Twenty-one-days post germination (DPG) plants exposed to 250 mJ of UV-C irradiation were kept in a growth room for 72 h and thereafter documented together with rosette leaves of plants not exposed to UV-C (control). Scale bar = 2 cm.
(B) The level of remaining chlorophyll in the first seven leaves (oldest to youngest from left to right) after exposing WT and the various mutant plants to UV-C treatment.
(C) Indicated aldehyde profiling in control (blue bars) and UV-C treated (red bars) plants. Leaves from three different plants were taken as one replica, and the bars show the average of at least four replicas. *aao3Ss* represents the average of the three independent *aao3* single mutants.
(D) Aldehyde oxidase 3 (AAO3) in gel activity in control and UV-C treated WT, *aao2* [(KO-95), SAIL_563_G09 (KO-563)], and *aao3Ss* (*aao3S-1*, *aao3S-12*, *aao3S-18*) using abscisic aldehyde as the specific substrate for AAO3. 150 μg crude protein extracted from WT, *aao2* (KO-95 and KO-563), and *aao3Ss* (*aao3S-1*, *aao3S-12*, *aao3S-18*) rosette leaves was fractionated by NATIVE PAGE and were used for activity. The gels were scanned after 30 min, and the intensity of the activity bands was estimated using ImageJ software (http://imagej.nih.gov/ij/) and compared with that obtained with UV-C untreated (control) WT (employed as 100%) and presented as relative intensity (RI).
(E) Abscisic acid (ABA) level in rosette leaves of WT, *aao2KO* (*KO-95*, *KO-563*), *aao1S* (*aao1S-11*), and *aao3Ss* (*aao3S-1*, *aao3S-12*, *aao3S-18*) untreated control (blue bars) and UV-C treated (red bars) plants. Different letters above the bar indicate significant differences (Tukey–Kramer HSD test, $P < 0.05$). Asterisk shows significant differences between treatments within the same genotype (Student's *t* test, $P < 0.05$).

was followed by AAO2 activity decrease in WT, *aao1KO*, and *aao3KO* plants. Accordingly, the absence of AAO2 in *aao2KO* plant resulted in higher activity of AAO3 and/or AAO1, and thus a better aldehyde detoxification and reduced chlorophyll degradation (Figure 4A–D).

The absence of active AAO2 enhances tolerance to UV-C irradiation and Rose-Bengal application by improving the capacity of AAO3 to detoxify aldehydes

The higher resistance of *aao2KO* mutants compared to WT exposed to UV-C irradiation and Rose-Bengal application prompted us to examine the possible role of each of the two enzymes: AAO1 and AAO3, in the improved tolerance to the stresses by generating single functioning mutants. The generation of single functioning *aao1* (*aao1S*) was done by silencing *AAO3* in the background of *aao2* (KO-95), while *aao3Ss* was generated by silencing *AAO1* in the background of *aao2* (KO-95) or *AAO2* silencing in the background of *aao1* KO mutant. The AAO-compromised lines were exposed to UV-C irradiation or Rose-Bengal spray after verifications of the mutations by detection of the transcript's expression of the targeted genes as compared to the expression in WT leaves (Figure S7).

Notably, rosette leaves of the *aao1S* (*aao1S-11*) mutants impaired in AAO3 and AAO2 expressions exhibited significantly lower remaining chlorophyll levels than WT leaves 3 days after exposing to 250 mJ of UV-C irradiation or 0.05 mM of Rose-Bengal application. In contrast, *aao3Ss* mutants (*aao3S-1*, *aao3S-7*, *aao3S-12*, *aao3S-18*) impaired in AAO1 and AAO2 expression, as well as the *aao2* (KO-95) mutant exhibited significantly higher remaining chlorophyll level than WT in response to the applied stresses (Figures 5A,B and 6A,B). Further, the detection of aldehydes level in rosette leaves was carried out 3 days after the UV-C irradiation and revealed significantly higher levels of benzaldehyde, crotonaldehyde, propionaldehyde, and HNE in WT leaves compared to *aao2KO* and the three *aao3Ss* (*aao3S-1*, *aao3S-12*, *aao3S-18*) mutants. In contrast, the levels of these aldehydes in *aao1S* mutant leaves were similar to those in WT (Figure 5C). Detection of aldehydes content in leaves 17 h after Rose-Bengal application revealed significantly higher accumulation of acrolein,

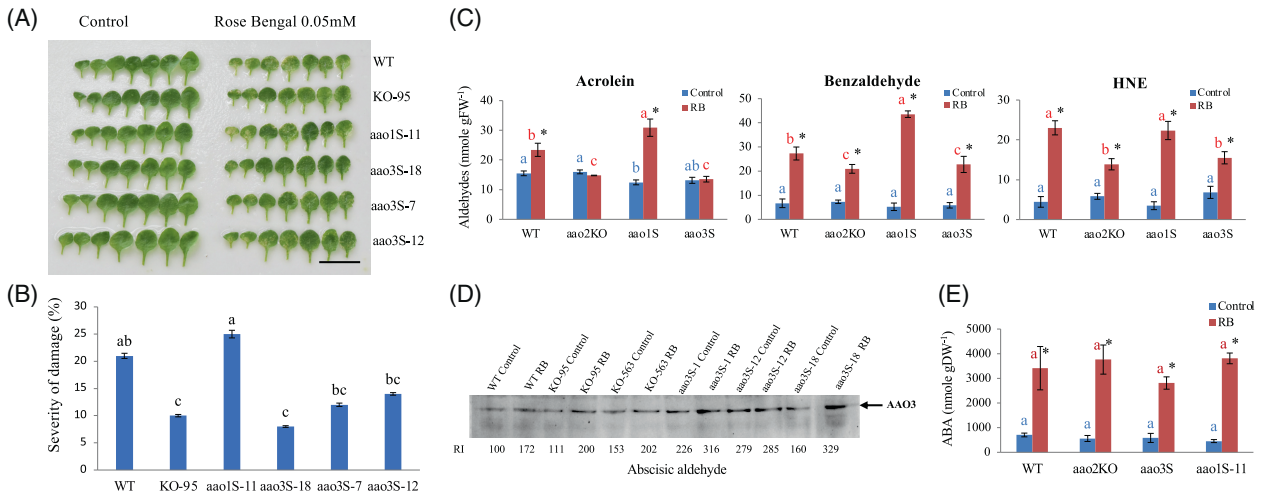

Figure 6. Determination of Rose-Bengal-induced senescence and senescence-related factors in rosette leaves of *Arabidopsis* aldehyde oxidases single mutants [*aao1Single* (*aao1S*) and *aao3Singles* (*aao3Ss*)], *aao2KO* [SALK_104895 (KO-95)], and wild-type (WT) plants.
(A) Representative photograph of WT, *aao2*, *aao1S*, and *aao3Ss* (*aao3S-7*, *aao3S-12*, *aao3S-18*) rosette leaves in untreated (control) and Rose-Bengal treated plants. 21-DPG plants treated with 0.05 mM of Rose-Bengal were kept in a growth room for 72 h and thereafter documented. Scale bar = 2 cm.
(B) Damage level in leaves as shown in (A) was calculated as described in "Experimental procedures" section. Means ± SEM (n = 6).
(C) Indicated aldehyde profiling in control (blue bars) and Rose-Bengal treated (red bars) plants. Seventeen hours after Rose-Bengal treatment leaves from three different untreated (control) or treated plants were taken as one replica, and the bars show the average of at least four replicas. *aao3Ss* is the average of the three independent *aao3* singles plants.
(D) Aldehyde oxidases 3 (AAO3) in gel activity in control and Rose-Bengal treated WT, *aao2* [(KO-95), SAIL_563_G09 (KO-563)], and *aao3Ss* using abscisic aldehyde as the specific substrate for AAO3. 150 μg crude protein extract from WT, *aao2* (KO-95, KO-563), and *aao3Ss* rosette leaves was fractionated by NATIVE PAGE and was used for the in-gel activity. The gels were scanned after 1 h, and the intensity of the activity bands was estimated using ImageJ software (http://imagej.nih.gov/ij/) and compared with that obtained with Rose-Bengal untreated (control) WT (employed as 100%) and presented as relative intensity (RI).
(E) ABA content in rosette leaves of WT, *aao2KO* (*KO-95*, *KO-563*), *aao1S* (*aao1S-11*), and *aao3Ss* (*aao3S-7*, *aao3S-12*, *aao3S-18*) untreated control (blue bars) and Rose-Bengal treated (red bars). Different letters above the bar indicate significant differences (Tukey–Kramer HSD test, $P < 0.05$). Asterisk shows significant differences between treatments within the same genotype (Student's t test, $P < 0.05$).

benzaldehyde, and HNE in WT and *aao1S* mutant leaves than in leaves of *aao2* (KO-95) and the *aao3Ss* (*aao3S-7*, *aao3S-12*, *aao3S-18*) mutants (Figure 6C). To further rule out the possible role of AAO1 in *aao2* resistance to the applied stresses, *AAO1* overexpression mutant (*A1OE*) used by us before (Nurbekova et al., 2021, figure 1b,c), was exposed together with WT plants to UV-C irradiation that revealed a higher chlorophyll degradation in A1OE (Figure S8A,B). Additionally, similar levels of benzaldehyde, crotonaldehyde, and HNE and higher levels of propionaldehyde in *A1OE* compared to WT were detected (Figure 3C). The results show better resistance of *aao2KOs* and *aao3Ss* mutants than WT, whereas *aao1S* and *A1OE* mutants exhibited similar resistance to WT when exposed to the abiotic stresses applied (Figures 5A–C and 6A-C; Figure S8). This indicates that AAO1 did not play a role in stress improved resistance of *aao2KO* as compared to WT while AAO3 is the major player in the detoxification of reactive aldehydes in the absence of active AAO2 in *aao2-KOs*. Additional support to this notion was demonstrated by employing ABal as the indicator substrate specific for AAO3 in-gel activity (Akaba et al., 1998, 1999; Koiwai et al., 2004; Koshiba et al., 1996; Nurbekova et al., 2021; Omarov et al., 1999; Seo, Koiwai, et al., 2000; Seo, Peeters, et al., 2000; Srivastava et al., 2017) that exhibited higher AAO3 activity level in response to UV-C or Rose-Bengal application in all the included genotypes, being significantly higher than WT in *aao2KO* and *aao3Ss* mutants. This result indicates that AAO3 is more active in the absence of active AAO2 in *aao2KO* and *aao3Ss* mutants compared to WT under the stresses applied (Figures 5D and 6D). Further detection of ABA levels revealed similar enhancement in WT as in *aao2KO*, *aao3S*, and *aao1S* mutant's rosette leaves exposed to UV-C or Rose-Bengal, indicating that enhanced aldehyde detoxification by higher AAO3 activity rather than differences in ABA level, played a significant role in the better resistance of *aao2KO* than in the WT or *aao1S* mutant (Figures 5E and 6E).

To examine if indeed *aao2KO* mutants can better resist toxic levels of aldehydes than WT, plants were exposed to 4.5 mM benzaldehyde as done recently (Nurbekova et al., 2021) and revealed higher chlorophyll degradation in WT than in the two independent mutants' leaves 72 h after aldehyde application (Figure S9A,B). These results further indicate the higher capacity of *aao2KO* mutants than WT to protect leaves from aldehyde-induced chlorophyll degradation.

DISCUSSION

The absence of active AAO2 improves AAO3's capacity to protect plants from UV-C and RB-induced chlorophyll degradation

Early observations showed the presence of three AAO genes in leaves and their expression dependency on the developmental stage and applied abiotic stresses. *Arabidopsis* AAO1 was shown to be mainly expressed in seedlings and rosette leaves (Koiwai et al., 2004; Seo, Koiwai, et al., 2000), oxidizing indole-3-carbaldehyde (ICHO) to indole-3-carboxylic acid [ICOOH (Bottcher et al., 2014)]. AAO3 was shown to be expressed in seedlings and rosette leaves (Koiwai et al., 2004; Seo, Koiwai, et al., 2000), oxidizing abscisic aldehyde (ABal) to abscisic acid (ABA) (Seo, Koiwai, et al., 2000; Seo, Peeters, et al., 2000) as well as protecting rosette leaves from stress-induced aldehyde toxicity by oxidizing the toxic aldehydes (Nurbekova et al., 2021). However, the roles of AAO2 are not known. In this study the role of AAO2 was investigated by exposing plants to Rose-Bengal spray or UV-C irradiation. Rose-Bengal is a well-known singlet oxygen generator (Havaux & Triantaphylides, 2009; Knox & Dodge, 1984) that participates in lipid peroxidation resulting in the generation of toxic aldehydes that above a certain level can lead to programmed cell death (Triantaphylides et al., 2008). Notably, treated WT plants exhibited stronger senescence symptoms (Figures 3A,B and 4A,B; Figures S1 and S4) than *aao2KOs* mutants in response to the applied stresses, the result of enhanced endogenously generated toxic aldehydes, such as acrolein, benzaldehyde, and HNE (Figures 3C and 4C). Interestingly, a decreased transcript expression of *AAO2* was noted, as well as declined AAO2 activity, parallel to the enhanced intensity of AAO1 and/or AAO3 (the most upper activity band), as well as the middle activity band [known as the heterodimer of AAO2 with AAO3 or AAO1 (Akaba et al., 1999; Koiwai et al., 2004)], in WT as well as in *aao1* and *aao3* mutant leaves exposed to UV-C irradiation (Figure S10; Figure 3D). Similar enhancement in AO activity of the heterodimers, as well as AAO3 and/or AAO1 activity, was noticed in WT as well as *aao1* and *aao3* mutants exposed to Rose-Bengal (Figure 4D). To verify whether AAO1 and/or AAO3 activity is responsible for the better resistance to the applied stresses in the absence of active AAO2, *aao1S* and *aao3Ss* mutants were exposed to UV-C irradiation or Rose-Bengal spray stresses together with WT and the *aao2KOs* mutant plants. Notably, exposing WT and *aao2KOs* mutants, as well as *aao1S* and *aao3S*s mutants to UV-C irradiation or Rose-Bengal spray, revealed that the enhanced senescence symptoms evident in WT and *aao1S* mutant but not in *aao2KOs* and *aao3Ss* (Figures 3A,B, 4A,B, 5A,B, and 6A,B; Figures S1 and S4) are the result of the presence of higher level of the toxic aldehydes, benzaldehyde, HNE, and acrolein in WT and *aao1S* compared to *aao3Ss and aao2KOs* mutant leaves (Figures 3C, 4C, 5C, and 6C). These results indicate the essentiality of the absence of active AAO2 and the presence of active AAO3, whereas the presence of active AAO1 is not essential for the better stress resistance of *aao2KO*, and the single mutants of *aao3Ss* under the applied stress conditions. The lower remaining chlorophyll content and higher level of propinaldehyde and similar enhancement in benzaldehyde, crotonaldehyde, and HNE levels in AAO1OE compared with WT upon UV-C irradiation further ruled out a possible involvement of AAO1 in *aao2KO* better resistance than WT (Figure S8). Employing in-gel AO assay with ABal as a specific substrate marker for AAO3 activity showed higher AAO3 activity in *aao2KOs* and *aao3Ss* as compared to WT leaves treated with UV-C or Rose-Bengal (Figures 5D and 6D), indicating that enhanced AAO3 capacity plays a role in *aao2KOs* and *aao3Ss* better resistance.

The involvement of reactive aldehydes in stress-induced damage to plants was previously reported, and among lipid peroxide-derived carbonyls, α, β-unsaturated aldehydes such as HNE, acrolein, and crotonaldehyde were identified as the most reactive species (Mano et al., 2010, 2014; Srivastava et al., 2017; Yamauchi et al., 2008). Interestingly, higher levels of benzaldehyde, acrolein, propionaldehyde, and crotonaldehyde were shown to induce early senescence in *aao3* leaves when exposed to UV-C irradiation. Similar to the experimental condition in the current study, *aao3* plants, known as ABA deficient mutants, were grown on half-strength MS media in agar plates sealed with surgical tapes, to control any drought involvement in senescence levels in WT and *aao3* mutant (Nurbekova et al., 2021). Indeed, under such controlled conditions no effect of ABA or drought stress was noticed in the *aao3* plants (Nurbekova et al., 2021), whereas similar levels of ABA were evident in WT, *aao2KOs*, *aao1S*, and *aao3Ss* in control and stressed plants (Figures 5E and 6E). To support the levels of ABA detected in the stressed plants the expression of *NCED3-2* gene was examined in the leaves of the control and the UV-C or Rose-Bengal stressed plants. Considering that *NCED3-2* gene product acts as the committed step of ABA biosynthesis (Ruggiero et al., 2004) generating xanthoxin that leads to the biosynthesis of ABAld, the substrate of AAO3 (Sussmilch et al., 2017), the similar transcript expression of *NCED3-2* evident in WT and *aao2KOs* and *aao3Ss* exposed to the applied stresses (Figure S11), is in agreement with the similar levels of ABA detected in the stressed genotypes. These results indicate that not the ABA level but rather the activated AAO3 is responsible for the higher level of the remaining chlorophyll by better aldehyde detoxification capacity in *aao2KOs* and *aao3Ss* mutant plants exposed to UV-C irradiation or Rose-Bengal application (Figures 5D and 6D).

The absence of active AAO2 in *aao2KO* mutants enhances AAO3 activity as the result of improved sulfuration by ABA3

The decrease in AAO2 activity in WT as well as the *aao1* and *aao3* mutants exposed to UV-C or Rose-Bengal (Figures 3D and 4D), and specifically the higher AAO3 activity than in WT, in the mutants absent active AAO2, the *aao2KOs* and *aao3SS*, grown with or without those stress conditions (Figures 5D and 6D), led us to examine the reason/s for such phenomenon. It is possible that the absence of AAO2 likely leads to higher availability of MoCo and/or less competition for MoCo sulfuration, resulting in increased activity in the upper activity band that includes AAO3 and AAO1 in WT and aao*2KOs* and only AAO3 in the *aao3SS*.

In vitro sulfuration of AO by employing Na_2S under anaerobic reducing conditions was previously demonstrated in leaves and roots of WT, recovering significantly the AO activity in the tomato Moco sulfurase (*flacca*) mutant roots and leaves (Sagi et al., 1999), as well as in the *Arabidopsis* Moco sulfurase (*aba3*) mutant, by employing L-Cysteine (Bittner et al., 2001; Mendel, 2022). Similarly, *in vitro* sulfuration was applied and in-gel activity assay of AAO using *trans*-2-nonenal as the substrate was carried out to examine AAO activity levels in the control and the sulfurated extracts of WT, *aao2KO*, and *aba3* leaves. Interestingly the uppermost activity band, containing enzyme activities of AAO1 and AAO3 (Nurbekova et al., 2021) was enhanced by 40% in control treated *aao2KO* mutant as compared to WT's most upper activity band. Notably, *in vitro* sulfuration of WT extracts resulted in a significant increase by 62% in AAO2 activity as well as more than twofold enhancement in the heterodimer middle activity band containing a monomer of AAO2, while the uppermost activity band exhibited a slightly lower activity level than the control when *trans-2*-nonenal was used as the substrate. In contrast, the *in vitro* sulfuration in *aao2KO* was almost twofold higher than in the sulfurated WT and 41% higher than the activity in the *aao2KO* control extract (Figure S12A). These results indicate that AAO2, as the homodimer (lowest migrated activity band) as well as the heterodimer (middle migrated activity band), targets the majority of the sulfuration as compared to the upper activity band (Figure S12A). In support of this notion, employing *in vitro* sulfuration in *aba3* mutant that lacks all AAO activities led to more than twofold higher intensity of AAO2 activity as compared to the heterodimer and the most upper activity bands of the sulfurated extract in *aba3* mutant [calculated using the intensities of the activity bands in *aba3* (Figure S12A)]. Importantly, the results indicated that the artificial sulfuration process used partially but significantly recovered AAO activities, as it was ca 60%, 90%, and 50% in the upper, middle, and lowest activity band as compared to the non-sulfurated extract of WT leaves, respectively (Figure S12A).

ABal that was shown as the specific substrate for AAO3 among the four aldehyde oxidases in *Arabidopsis* (Akaba et al., 1998, 1999; Koiwai et al., 2004; Koshiba et al., 1996; Seo, Koiwai, et al., 2000; Seo, Peeters, et al., 2000) was used to identify the responses of AAO3 to the sulfuration process, as one of the two enzymes responsible for the most upper activity band. Notably, while the sulfuration process recovered a faint AAO3 activity band in sulfurated *aba3* that was ca 11% of the activity detected in non-sulfurated WT under control conditions, the sulfuration of *aba3* after UV-C irradiation enhanced AAO3 activity by more than fivefold (Figure S12B), indicating that UV-C irradiation most likely enhanced the level of inactive unsulfurated AAO3 in *aba3* mutants. Since UV-C irradiation and environmental stress such as Rose-Bengal spray were shown to enhance the relative expression of *ABA3* transcription in WT and *aao2KOs* (Figure S13A,B) as well as the expression of *AAO3* transcript in WT but not in *aao2-KO* mutants (Figure S14), it is likely that UV-C will enhance the levels of active AAO3, at least in the *aao2KO* mutants mainly by sulfuration of inactive AAO3 proteins.

While control plants exhibited 150% higher AAO3 activity in *aao2KO* mutant compared to WT, the sulfuration process enhanced AAO3 activity in WT by 89% and in *aao2KO* by 37%, the latter still being higher than WT by 81%. Treating WT and *aao2KO* control plants with UV-C irradiation resulted in higher AAO3 activity by more than fourfold and twofold than in WT and *aao2KO control*, respectively. Notably, further sulfuration of the UV-C treated plants further enhanced AAO3 activity by 18% in WT and 14% in the mutant, the latter still higher than the WT by more than 8% (Figure S12B). These results indicate that while environmental stresses such as UV-C irradiation likely enhance the level of active AAO3 in both WT and the *aao2KO*, the active AAO2 in WT employs a sulfuration process essential for AAO3 activation, resulting in higher availability of activation by sulfuration of the AAO3 in *aao2KO* compared to AAO3 in WT.

In summary, the current study demonstrates that AAO2 activity level oppositely affects AAO3 activity, while mutation of *AAO2* expression better delays plant senescence by AAO3-enhanced aldehyde detoxification activity in plants exposed to UV-C irradiation or Rose-Bengal spray (Figures 1C–7). Firstly, it was shown that *aao2KO* can detoxify an array of reactive aldehydes by higher activity than in WT of AAO1 or AAO3 or both exposed to UV-C irradiation or Rose-Bengal spray. Additionally, it was shown that AAO3 and/or AAO1 activity increase was followed by AAO2 activity decrease in WT, *aao1KO*, and *aao3KO* plants exposed to UV-C radiation or Rose-Bengal spray compared to control untreated plants (Figures 3 and 4). Secondly, an essential interplay between AAO2 and

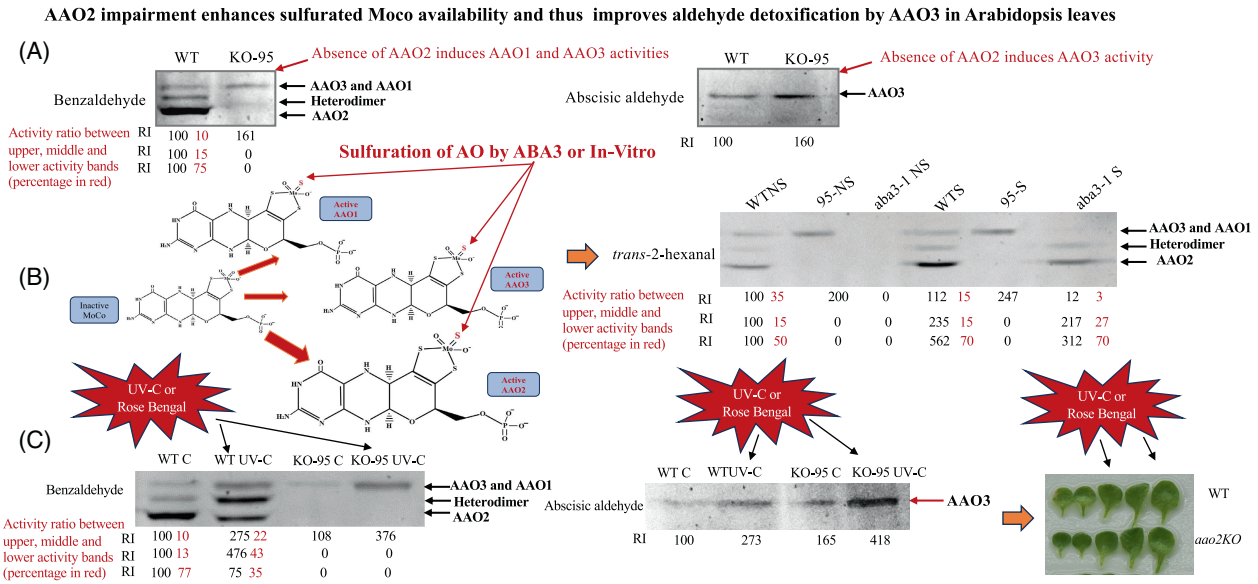

Figure 7. Schematic illustration describing how aldehyde oxidase 2 (AAO2) impairment enhances the availability of sulfurated molybdenum-cofactor (Moco) and enables improved aldehyde detoxification by AAO3 activity in *Arabidopsis* leaves.
(A) Demonstration of *Arabidopsis* AAOs activity assessment in WT and *aao2* [SALK104895 (KO-95)] mutant, using benzaldehyde or abscisic aldehydes as the substrate. Both activities demonstrate higher activity in *aao2* compared to the uppermost activity band in WT, whereas AAO2 activity is much higher than the lowermost AAO activity band in WT.
(B) The left-hand side illustrates that AAO2 is a major consumer of Moco sulfuration compared to AAO1 or AAO3. The right-hand side demonstrates how and why the absence of molybdenum cofactor sulfuration in AAO2 affects AAO's activity in WT, *aao2* mutant, and the molybdenum cofactor sulfurase (aba3-1, At1g16540) mutant plants. Accordingly, the *in vitro* sulfuration demonstrates that the uppermost activity band, the result of AAO1 and/or AAO3 activities, was enhanced by more than 23% over the control treated *aao2KO* mutant, and much higher compared to the effect of the sulfuration in WT's most upper activity band (12%).
(C) AAOs' activity in plants exposed to UV-C or Rose-Bengal application showed higher activity in AAO1 and/or AAO3 in *aao2KOs* than in WT leaves when using benzaldehyde as the substrate and enhanced AAO3 when using abscisic aldehyde (the specific substrate of AAO3), resulting in less senescence symptoms in *aao2KOs*, demonstrating the essential role of AAO2 expression level in regulating AAO3 activity.

AAO3 in the regulation of senescence level and carbonyl aldehyde detoxification under stress conditions was presented. Delayed senescence and the lower toxic aldehyde levels in stress-treated *aao2KO* and *aao3Ss* mutants, but not in WT, *aao1S*, and *AAO1OE* mutants, demonstrate the essentiality of AAO2 impairment to plant senescence delay by enhancing aldehyde detoxification activity by AAO3 (Figures 5 and 6). It was also shown that the absence of active AAO2 leads to higher availability of sulfurated MoCo, resulting in increased activity of AAO3 in *aao2KOs*. Firstly, it was shown that the AAO2 is responsible for most of the total AAO activity band intensities in unstressed WT leaves [Figure 7A most left insert (see in red a description and % level of each of the three activity bands)], thus employing the majority of the active sulfurated Moco (Figure 7B, left side). This resulted in ca 60% enhanced AAO3 activity in *aao2KO* compared to WT (detected by abscisic aldehyde, the specific substrate for AAO3) [*KO-95* (Figure 7A, right insert)]. Accordingly, AAO2 in *aba3-1* crude protein which normally does not show any AAO activity, after sulfuration *in vitro*, was similar to the AAO2 in WT activity bands occupying the major AO activity (70% of the total), indicating the high consumption of the sulfuration components by AAO2 (Figure 7B, right insert, Figure S12A). Finally, the application of the UV-C irradiation or Rose-Bengal spray resulted in enhanced benzaldehyde-dependent activity of the most upper activity band (AAO1 and AAO3) as compared to the control unstressed WT leaves. Yet, such activity level was much higher in the absence of AAO2 in the stressed *aao2KO* mutant leaves (Figure 7C, left insert), the result of enhanced Moco sulfuration (Figure S12B). Employing abscisic aldehyde, the specific substrate of AAO3 revealed a much higher stress-induced increase in AAO3 activity in the absence of AAO2 (Figure 7C, middle insert) resulting in lower chlorophyll degradation, the result of better detoxification of toxic aldehydes by AAO3 in mutant leaves (Figure 7C, right insert). These results indicate that the AAO2 protein consumes Moco sulfuration resources essential to AAO3 activity, thus limiting the plant's capacity to detoxify aldehydes generated in response to UV-C or Rose-Bengal application, and therefore, resulting in accelerated senescence in WT compared to *aao2KOs* and *aao3Ss* mutants.

EXPERIMENTAL PROCEDURES

Chemicals

Acrolein, benzaldehyde, cinnamaldehyde, citral, crotonaldehyde, decanal, dodecanal, heptaldehyde, hexanal, *trans*-2-heptenal, 4-hydroxynonenal-dimethylacetal (HNE-DMA), indole-3-carboxaldehyde, malondialdehyde [tetrabutylammonium salt], 1-naphthaldehyde, nonanal, *trans*-2-nonenal, propionaldehyde, salicylaldehyde, *trans*-2-pentanal, *trans*-2-hexanal, vanillin, diphenyltetrazolium bromide (MTT), and phenazine methosulfate (PMS) were purchased from Sigma Aldrich Chemical Company Inc. Abscisic aldehyde was purchased from Toronto Research Chemicals (www.trc-canada.com).

Plant material and growth conditions

Arabidopsis thaliana var. Columbia wild type (WT), T-DNA homozygous knockout (KO) lines for *AAO3* (At2g27150), SAIL_78_H09 (KO9), *AAO1* (At5g20960, SALK_018100), and *AAO2* (At3g43600), KOs SALK_104895 (KO-95), and SAIL_563_G09 (KO-563) were procured from ABRC (http://abrc.osu.edu/). *aba3-1* (At2g16540) used in this study and used by us before (Bekturova et al., 2021; Sagi et al., 2002) was procured from the same source. Homozygous lines of T-DNA KOs were screened using PCR with specific sets of primers (Table S1A). *aao1S* (*aao1* single) mutant was generated by silencing *AAO3* in the background of *aao2* (KO-95), and *aao3Ss* was generated by silencing *AAO1* in the background of *aao2*(KO-95) *and* silencing *AAO2* in the background of *aao1* (*KO-a1-100*). The expression of *AAO* genes was quantified by qPCR (Figure S7) in *aao1S* and *aao3Ss* mutants by employing forward and reverse primers localized to either side of the T-DNA insertion.

For the gene silencing we used the RNA interference system as done by us before (Brychkova et al., 2007; Yarmolinsky et al., 2013; Yesbergenova et al., 2005). The sense fragment was ligated into pRNA69 plasmid via the restriction sites XhoI and EcoRI, and the antisense fragment through the restriction sites BamHI and XbaI. The resulting construct was digested, and the fragment containing the CaMV 35S promoter and the inserted *AAO* fragments was inserted via Not1 flanking sites of the binary vector pML-BART.

The generation of *AAO1*, *AAO2*, and *AAO3* fragments for the ligation into pRNA69 plasmid was amplified employing the primers listed below using cDNA specimens as templates (see description of cDNA preparation in "RNA isolation, cDNA preparation, and real-time PCR" section). For *AAO1* silencing the Forward primer was ATTggatccctcgagCGAGTTCTTCGGATCTTTA containing BamHI and XhoI (respectively, underlined in small letters) and the Reverse primer was GCCtctagagaattcAACATTCTGATCAAAACCA containing Xba1 and EcoR1 (respectively, in small letters). The sense fragment in pRNA69 included the XhoI/EcoRI fragment and the antisense contained the XbaI/BamHI fragment, each containing 94 nucleotides of *AAO1* cDNA (Table S4). For *AAO2* silencing the Forward primer was ATTctagactcgagTCTTGAGGCTCATGAT containing Xba1 and XhoI (respectively, in small letters) and the Reverse primer was AGGggatccgaattcTTCAGAGTTTGTTTCA containing EcoRI and BamHI (respectively, in small letters). The sense fragment in pRNA69 included the XhoI/EcoRI fragment and the antisense contained the XbaI/BamHI fragment, each containing 67 nucleotides of *AAO2* cDNA (Table S4). For *AAO3* silencing the Forward primer was ATTctagactcgagGAAAGAGAAGGTTGATAAT containing Xba1 and XhoI (respectively, in small letters) and the Reverse primer was AGGggatccgaattcTGTTATGAAGCTCAG containing EcoRI and BamHI (respectively, in small letters). The sense fragment in pRNA69 included the XhoI/EcoRI fragment and the antisense contained the XbaI/BamHI fragment, each containing 81 nucleotides of *AAO3* cDNA (Table S4).

The constructs were introduced into *Agrobacterium tumefaciens* strain GV3101 as described before (Brychkova et al., 2007; Srivastava et al., 2017) and transformed into the KO mutants using the floral dip method (Clough & Bent, 1998). Transformed *Arabidopsis* lines were first selected by resistance to Basta® (glufosinate ammonium: Aventis CropScience https://www.bloomberg.com) and verified by transcript expression level and sequencing.

Seeds were sown in Petri dishes containing half-strength MS medium supplemented with 0.5% plant Agar (https://www.duchefa-biochemie.com/) and were placed at 4°C for 2 days for stratification and then were grown at 14 h light/10 h darkness in a growth room, 22°C, with 75%–85% relative humidity, and 100–150 μmol m^{-2} sec^{-1} as described in Brychkova et al. (2007). Seven days post germination (DPG), the plants were transferred to 90 mm plates containing half-strength MS medium supplemented with 0.5% sucrose and 1% agar. The biomass of the rosette leaves was determined 3 or 4 days after UV-C irradiation or 17 h after spraying plants with RB. Untreated plants were used as the control.

RNA isolation, cDNA preparation, and real-time PCR

To quantify the transcripts using quantitative reverse transcriptase-polymerase chain reaction (qPCR), total RNA was prepared by using the Aurum™ total RNA Mini Kit (Bio-Rad, Hercules, CA) according to the manufacturer's instructions. The cDNAs were prepared in a 10 μL volume containing 350 ng of plant total RNA that was reverse-transcribed with an iScript™ cDNA Synthesis Kit using modified MMLV-derived reverse transcriptase (Bio-Rad), a blend of oligo-d(T) and random hexamer primers according to the manufacturer's instructions. The generated cDNA was diluted 10 times, and the quantitative analysis of transcripts was performed employing the sets of primers enlisted in Table S2A as described before (Brychkova et al., 2007; Oshanova et al., 2021).

DNA sequence analysis

Sequence analysis was performed with the ABI Prism Big Dye Terminator Cycle Sequencing Ready Reaction Kit on an ABI Prism 310 cycle sequencer (PE Applied Biosystems, Warrington, UK).

Identification of unique peptides in activity bands

To confirm the identity of the AAOs involved in the formation of the lower (most migrated) bands in WT, *aao1*, and *aao3* KO, during aldehyde oxidation (Figure 1C), the activity bands were excised from the native gel, and fractionated with 12% SDS-PAGE. Thereafter the proteins were stained by Coomassie Brilliant Blue, and the individual lanes harboring stained bands were cut from the gel and sent for peptide sequencing at The Smoler Protein Research Center (https://proteomics.net.technion.ac.il/). The proteins were trypsinized, and the resulting peptides were separated by HPLC and analyzed by LC-S/MS on Q-Exactive (Thermo Fisher Scientific). Data analysis was done as described in Kurmanbayeva et al. (2017) and Nurbekova et al. (2021).

Protein extraction and fractionation

Soluble proteins were extracted from *Arabidopsis* rosette leaves as described before (Sagi et al., 1998). Concentrations of total soluble protein in the resulting supernatant were determined

according to Bradford (1976). Native PAGE was carried out as follows: samples were subjected to a Bio-Rad Mini-Protean III slab cell (Bio-Rad, Richmond, CA, USA), with a discontinuous buffer system (Laemmli, 1970) in 7.5% (w/v) polyacrylamide separating gels and 4% (w/v) stacking gels in the absence of SDS at 4°C. Tissue/buffer ratio was 1:3 (weight/volume). Extracted crude protein samples were centrifuged at 15 000*g* for 20 min at 4°C and then loaded to the gel after equalization of the proteins. The native-PAGE was carried out using 1.5 mm thick slabs loaded with indicated levels of proteins.

AAO in-gel activity

AAO activity was tested using different aldehydes in 50 mM Tris-HCl, pH 7.5, containing 1 mM 3-(4,5-dimethylthiazol-2-yl)-2,5-diphenyltetrazolium bromide (MTT), 0.1 mM phenazine methosulfate (PMS), and one of various aldehydes (concentration is mentioned at the required places). The reactions were stopped by immersion of the gels in 5% acetic acid. The quantity of resulting formazan activity bands was directly proportional to enzyme activity during a given incubation time, in the presence of excess substrate and tetrazolium salt (Rothe, 1974). The gels were scanned, and the intensity of the bands was determined using ImageJ software (http://imagej.nih.gov/ij/).

Western blot analysis

Proteins were extracted in buffer containing 250 mM Tris-HCl (pH 8.48), 1.25 mM EDTA, 14 mM GSH, 4 mM dithiothreitol, 5 mM L-Cys, 0.5 mM sodium molybdate, and 400 mM Suc. Lanes were loaded with 0.5, 10, or 25 μg crude protein in each lane for the detection of Rubisco, D1, or AAO4, respectively. The loaded proteins were separated in 12.5% (w/v) acrylamide gels by SDS-PAGE followed by transfer to polyvinylidene difluoride membranes. Commercial anti-D1 protein of PSII (AS05 084) primary antibodies produced by Agrisera AB was used in dilutions of 1:10 000. Antibodies recognizing the large subunits of Rubisco, a gift from Prof. Michal Shapira (Life Science Department, Ben-Gurion University of the Negev, Israel), was used in dilution of 1:20 000. The detection of AAO4 protein expression in WT siliques, as well as WT and *aao2KO* mutant's rosette leaves was done by using a specific antibody raised against an AAO4 synthetic polypeptide CNAGRHEKLRMGEYLVS as described previously (Srivastava et al., 2017). The blots were visualized using Gel-Doc (Bio-Rad) after staining with ECL detection system (Clarity™ Western ECL substrate, Bio-Rad, www.bio-rad.com), according to the manufacturer's instructions.

In vitro sulfuration of crude extracts

In vitro sulfuration was carried out as previously described (Sagi et al., 1999, 2002) with slight modifications. Protein extraction of rosette leaves was done as described above in "Experimental procedures" section. The high heat stability of plant MoCo-containing hydroxylases in plant leaves (Bower et al., 1978; Omarov et al., 1999; Sagi et al., 1999) allowed to heat the resulted supernatant for 90 sec at 65°C and additionally centrifuge for 10 min at 4°C as done previously (Nurbekova et al., 2021). Five hundred microliter supernatant of the leave extracts as well as 1 mL of extraction buffer passed through G-25 Sephadex that was previously equilibrated with 6 mL extraction buffer and 1 mL of the desalted protein was collected. For the sulfuration process 450 μL of the desalted protein incubated at room temperature for 40 min together with 20.25 μL 0.1 M dithionite, 17 μL of 0.5 M Na_2S, and 22.5 μL of 1.25 mM methyl viologen was the indicator of the reducing conditions, while gently flushing N_2 through the mixture to maintain anaerobic conditions. A volume of 59.75 μL extraction buffer was added to 450 μL desalted protein that served as the control. Proteins were equalized before and after sulfuration, and AO activity was detected in polyacrylamide gels by staining after native electrophoresis as previously described. Detection of AO activity was carried out with desalted proteins extracted from WT, *aao2KO*, and *aba3-1* mutant leaves.

UV-C (254 nm) irradiation

UV-C treatment was applied by subjecting equal age plants (21–23 DPG) to 250 mJ UV-C irradiation of 254 nm during 90 sec, using CL 508 Crosslinkers (UVITec Ltd, UK) as done by us before (Nurbekova et al., 2021; Soltabayeva et al., 2022). Plants were transferred to the normal growth room condition immediately after UV-C irradiation. WT, *aao2* (KO-95 and KO-563), *aao1S* (*aao1S-11*), and *aao3Ss* (*aao3S-1*, *aao3S-12*, *aao3S-18*) mutant plants, grown in 1% agar plates containing half-strength MS media and 0.5% sucrose. UV-C irradiation-treated and untreated (control) plants were placed in the controlled growth room. Photographs of the plants were taken 3 or 4 days after UV-C irradiation, and the remaining plants were frozen in liquid N and then stored at −80°C for further use.

Rose-Bengal treatment in rosette leaves

Twenty-three-day-old *aao2KOs* SALK_104895 (KO-95) and SAIL_563_G09 (KO-563), WT, *aao1S* (*aao1S-11*), and *aao3Ss* (*aao3S-7*, *aao3S-12*, *aao3S-18*) plants, grown 3 plants per 90 mm plate, were used for Rose-Bengal treatment. Rose-Bengal was dissolved using a magnetic stirrer in DDW containing 0.01% Silwet L-77. Fifty μM Rose-Bengal was sprayed onto the plates containing plants, the remaining solution was removed carefully, and plates were resealed with surgical tape and kept 1 h under the dark and then were transferred to the normal growth room condition. DDW containing 0.01% Silwet L-77 was used as the control. Plants were sampled 17 h after Rose-Bengal application. The effect of Rose-Bengal treatment was documented 72 h after the Rose-Bengal application unless mentioned otherwise.

Chlorophyll and leaf-damage level determination

Total chlorophyll content was measured in extracts of the rosette leaves as described before (Graan & Ort, 1984). The values for remaining chlorophyll content in rosettes were determined as the quantity of chlorophyll per 20 mg for each sample divided by the quantity of chlorophyll per 20 mg mock (control untreated) and were expressed as remaining chlorophyll (%). The severity of leaf damage after Rose-Bengal treatment was as follows: 0, no damage; (1) 1%–5%; (2) 6%–10%; (3) 11%–25%; (4) 26%–40%; (5) >41% of leaf area damaged. The average leaf damage was then multiplied by the total number of damaged leaves to determine the level of damage as shown in Brychkova et al., 2008.

Determination and quantification of aldehydes, determination of aldehyde toxicity, and ABA determination

Rosette leaves (250 mg) were immersed in 2.5 mL acetonitrile (all acetonitrile mentioned is of HPLC Ultra Gradient Solvent) containing 25 nmol 2-ethylhexanal (as an internal standard) and 0.005% (w/v) butylhydroxytoluene (BHT). The leaves were incubated in a screw-capped glass tube at 60°C for 30 min, and the supernatant was collected by decantation. For derivatization of aldehydes, 2,4-dinitrophenylhydrazine (DNPH) was purified (recrystallized) as described before (Mano & Biswas, 2018). Briefly, an equal of

commercial DNPH was dissolved in 50 mL of warm (60°C) acetonitrile. Complete dissolved DNPH was chilled gradually (for several hours), and generated crystals were collected through filter paper. DNPH crystals were dissolved in acetonitrile to make 20 mM solution. To derivatize aldehydes with DNPH, 62.5 μL of 20 mM DNPH (in acetonitrile) and 48.4 μL of 99% formic acid (LC–MS quality) were added to the resulting supernatant and incubated at 25°C for 60 min. Thereafter 2.5 mL NaCl (5 M) and 450 mg $NaHCO_3$ were added to the mixture for neutralizing formic acid and the mixture was shaken at intervals for 10 min. After centrifugation, the upper layer was collected and dried in vacuum and then dissolved in 250 μL acetonitrile. This solution was applied on a Bond Elute C18 cartridge [sorbent mass 200 mg (Agilent Technologies, USA)], which has been pre-washed with 2 mL acetonitrile, and the pass-through (250 μL) and subsequent wash (150 μL acetonitrile) were combined as the eluted solution. Fifteen microliter of the eluted solution were analyzed using Thermo Scientific Dionex UltiMate 3000 UHPLC system (http://www.dionex.com/en-us/products/liquid-chromatography/lc-systems/lp-87043.html) with Variable Wavelength VWD-3100 detector. The 15 μL eluted solution was injected into a Wakosil DNPH-II column (4.6 mm × 150 mm (W), No. 17193, Wako Pure Chemical Industries, Ltd., Osaka, Japan, http://www.wako-chem.co.jp/english) with the following elution conditions: 1 mL min^{-1} flow rate, 0–5 min, 100% HPLC quality Eluent A (Wako Pure Chemical Industries) 5–20 min, a linear gradient from 100% A to 100% HPLC quality Eluent B (Wako Pure Chemical Industries); 20–25 min, 100% B, 25–45 min, a linear gradient from 100% B to 100% C (acetonitrile). The detection wavelength was 340 nm, and the column temperature was 35°C.

Aldehydes were identified by their retention time which correspond with its own standards and their contents were determined by dividing the peak area of aldehyde by the peak area of the internal standard detected for each plant sample at the same run according to Matsui et al. (2009), Yin et al. (2010), Biswas and Mano (2015), as well as Biswas et al. (2019), as shown recently by us (Bekturova et al., 2021; Nurbekova et al., 2021; Srivastava et al., 2017). The content of the aldehydes was calculated from the peak area of the corresponding DNP-carbonyl, peak area of internal standard, conversion factor k for each aldehyde, and exact molecular weight for each sample, using appropriate software [CHROMELEON7 (https://www.thermofisher.com)].

Importantly, the currently presented retention time (Figures S2, S3, S5, S6, S15 and S17) corresponded with our previously published data (figures S7A,B, S14, S16 in Nurbekova et al., 2021) and with results published by others (see figure 7 in Yin et al., 2010 and figure 3a in Biswas & Mano, 2015). Aldehyde toxicity was examined with 21-day-old *aao2KOs* and WT plants as done by us before [Nurbekova et al., 2021 (see the current Figure S17 related to benzaldehyde toxicity shown in figure 5 in Nurbekova et al., 2021)]. ABA concentrations in leaves were determined as previously described (Turečková et al., 2009).

Preparation of DNP-aldehyde standards

DNP-aldehyde standards were prepared as previously described (Mano & Biswas, 2018). 1 mM of DNPH (ca. 0.3 g) was dissolved in 20 mL acetonitrile (HPLC Ultra Gradient Solvent). To the dissolved DNPH solution, 1 mM of aldehyde and a few drops of formic acid were added. The mixture was kept under a chemical hood by stirring. For acetals, such as acrolein, 1 mmol of aldehyde was dissolved in 30 mL of DNPH solution (5 mM in 2 M HCL). After DNP-aldehyde precipitation, crystals of DNP-aldehyde standards were collected and dried. The mol amount of DNP-derivative was determined by the weight.

ACCESSION NUMBERS

Sequence data used in this work can be found in the GenBank/EMBL data libraries under accession numbers At2g27150 (AAO3), At3g43600 (AAO2), and At5g20960 (AAO1).

AUTHOR CONTRIBUTIONS

ZN participated in designing the research plans and performed the experiments and analysis; SS read and commented on the manuscript; ZDN participated in in-gel activity and Western blot analysis, KK, JP, BC, and DS participated in Western blot and qPCR analysis. VT and MSt performed the detection of ABA level; EZ-Z and RO read and commented on the manuscript; MS conceived the original idea, designed the research plan, and supervised the research work. The article was jointly written by ZN and MS.

ACKNOWLEDGMENTS

MS thankfully acknowledge a grant from the Israel Center of Research Excellence (Plant Adaptation grant no. 757/12), and MSt and VT thankfully acknowledge a grant from the European Regional Development Fund-Project (no. CZ.02.1.01/0.0/0.0/16_019/0000827).

CONFLICT OF INTEREST STATEMENT

All authors have no conflicts of interest to declare.

SUPPORTING INFORMATION

Additional Supporting Information may be found in the online version of this article.

Table S1. Verification of AAO2 (At3g43600) KO mutants (KO-95 and KO-563) homozygosity.

Table S2. (A) Details of primers used to carry out quantitative real-time PCR analysis and (B) the results of sequence analysis of the resulting product of AAO2 and aba3.

Table S3. Unique peptides of *Arabidopsis* aldehyde oxidases (AAOs) identified by LC–MS.

Table S4. List of cDNA fragments with the primers (underlined without the restriction sites) used for generating the AAOs RNAi plants.

Figure S1. Immunoblotting analysis of chlorophyll-related proteins in wild-type (WT), *aao2KOs* [SALK_104895 (KO-95) and SAIL_563_G09 (KO-563)] mutant plants in response to the UVC irradiation.

Figure S2. HPLC chromatogram for aldehydes estimation in WT and KO-563 mutant exposed to UV-C irradiation.

Figure S3. HPLC chromatogram for aldehydes estimation in WT and KO-95 mutant exposed to UV-C irradiation.

Figure S4. Immunoblotting analysis of chlorophyll-related proteins in wild type (WT). *aao2KOs* [SALK_104895 (KO-95) and SAIL_563_G09 (KO-563)] mutant plants in response to Rose-Bengal application.

Figure S5. HPLC chromatogram for aldehydes estimation in WT and KO-563 mutant exposed to Rose-Bengal application.

Figure S6. HPLC chromatogram for aldehydes estimation in WT and KO-95 mutant exposed to Rose-Bengal application.

Figure S7. Relative transcript expression of AAO1(At5g20960), AAO2 (At3g43600), and AAO3 (At2g27150) in rosette leaves of 23-days post germination *Arabidopsis* WT, *aao1Single* (*aao1S*) and independent *aao3Singles* (*aao3Ss*) mutant plants.

Figure S8. Determination of UV-C-irradiation-induced senescence and senescence-related factors in rosette leaves of *Arabidopsis* wild-type (WT) and AAO1 overexpression (AAO1OE) mutant plants.

Figure S9. The effect of exogenously applied benzaldehyde on rosette leaves of wild-type (WT) and *aao2KO* [SALK_104895 (KO-95) and SAIL_563_G09 (KO-563)] mutant plants.

Figure S10. Relative transcript expression of *AAO2* (At3g43600) and aldehyde oxidases (AAOs) activity in control and UV-C treated WT, *aao2* [SALK_104895 (KO-95)], *aao1* [At5g20960, SALK_018100, (a1-100)], and *aao3* [At2g27150, SAIL_78_H09 (KO9)] mutant plants.

Figure S11. The effect of UV-C irradiation or Rose-Bengal (RB) on the transcript expression of *Nine-cis-epoxy carotenoid dioxygenase 3* (*NCED3-2*; At3g14440) gene in rosette leaves of *Arabidopsis* WT and *aao2KO* [SALK_104895 (KO-95) and SAIL_563_G09 (KO-563)] mutant plants.

Figure S12. The effect of molybdenum cofactor sulfuration *in vitro*, and UV-C irradiation on aldehyde oxidases (AAOs) activity in WT, *aao2* [SALK_104895 (KO-95)], and the molybdenum cofactor sulfurase (*aba3-1*, At1g16540) mutant plants.

Figure S13. The effect of UV-C irradiation or Rose-Bengal application on the transcript expression of *ABA3* (At1g16540) in rosette leaves of *Arabidopsis* WT, and *aao2* [SALK_104895 (KO-95) and SAIL_563_G09 (KO-563)] mutant plants.

Figure S14. The effect of UV-C irradiation or Rose-Bengal application on the transcript expression of *AAO3* (At2g27150) in rosette leaves of *Arabidopsis* WT and *aao2* [SALK_104895 (KO-95) and SAIL_563_G09 (KO-563)] mutant plants.

Figure S15. HPLC chromatogram for acetaldehyde, acrolein, crotonaldehyde, HNE standards together with reactive carbonyl species extracted from WT plant.

Figure S16. HPLC chromatogram for propionaldehyde, crotonaldehyde and benzaldehyde standards together with reactive carbonyl species extracted from WT plant.

Figure S17. HPLC chromatogram for benzaldehyde standard together with WT and *aao3* mutant exposed to benzaldehyde application.

REFERENCES

Akaba, S., **Leydecker, M.T.**, **Moureaux, T.**, **Oritani, T.** & **Koshiba, T.** (1998) Aldehyde oxidase in wild type and aba1 mutant leaves of *Nicotiana plumbaginifolia*. *Plant & Cell Physiology*, **39**, 1281–1286. Available from: https://doi.org/10.1093/oxfordjournals.pcp.a029331

Akaba, S., **Mitsunori, S.**, **Dohmae, N.**, **Takio, K.**, **Sekimoto, H.**, **Kamiya, Y.** ***et al.*** (1999) Production of homo- and hetero-dimeric isozymes from two aldehyde oxidase genes of *Arabidopsis thaliana*. *Journal of Biochemistry*, **126**, 395–401. Available from: https://doi.org/10.1093/oxfordjournals.jbchem.a022463

Bekturova, A., **Oshanova, D.**, **Tiwari, P.**, **Nurbekova, Z.**, **Kurmanbayeva, A.**, **Soltabayeva, A.** ***et al.*** (2021) Adenosine 5′ phosphosulfate reductase and sulfite oxidase regulate sulfite-induced loss in *Arabidopsis*. *Journal of Experimental Botany*, **72**, 6447–6466. Available from: https://doi.org/10.1093/jxb/erab249

Bindschedler, L.V. & **Cramer, R.** (2011) Quantitative plant proteomics. *Proteomics*, **11**, 756–775. Available from: https://doi.org/10.1002/pmic.201000426

Biswas, M.S., **Fukaki, H.**, **Mori, I.C.**, **Nakahara, K.** & **Mano, J.** (2019) Reactive oxygen species and reactive carbonyl species constitute a feed-forward loop in auxin signaling for lateral root formation. *The Plant Journal*, **100**, 536–548. Available from: https://doi.org/10.1111/tpj.14456

Biswas, M.S. & **Mano, J.** (2015) Lipid peroxide-derived short-chain carbonyls mediate hydrogen peroxide-induced and salt-induced programmed cell death in plants. *Plant Physiology*, **168**, 885–898. Available from: https://doi.org/10.1104/pp.115.256834

Biswas, M.S. & **Mano, J.** (2016) Reactive carbonyl species activate caspase-3-like protease to initiate programmed cell death in plants. *Plant & Cell Physiology*, **57**, 1432–1442. Available from: https://doi.org/10.1093/pcp/pcw053

Bittner, F., **Oreb, M.** & **Mendel, R.R.** (2001) ABA3 is a molybdenum cofactor sulfurase required for activation of aldehyde oxidase and xanthine dehydrogenase in *Arabidopsis thaliana*. *The Journal of Biological Chemistry*, **276**, 40381–40384. Available from: https://doi.org/10.1074/jbc.C100472200

Bottcher, C., **Chapman, A.**, **Fellermeier, F.**, **Choudhary, M.**, **Scheel, D.** & **Glawischnig, E.** (2014) The biosynthetic pathway of indole-3-carbaldehyde and indole-3-carboxylic acid derivatives in *Arabidopsis*. *Plant Physiology*, **165**, 841–853. Available from: https://doi.org/10.1104/pp.114.235630

Bower, P., **Brown, H.** & **Purves, W.** (1978) Cucumber seedling indole acetaldehyde oxidase. *Plant Physiology*, **61**, 107–110. Available from: https://doi.org/10.1104/pp.61.1.107

Bradford, M.M. (1976) A rapid and sensitive method for the quantitation of microgram quantities of protein utilizing the principle of protein-dye binding. *Analytical Biochemistry*, **72**, 248–254. Available from: https://doi.org/10.1016/0003-2697(76)90527-3

Brychkova, G., **Alikulov, Z.**, **Fluhr, R.** & **Sagi, M.** (2008) A critical role for ureides in dark and senescence-induced purine remobilization is unmasked in the *Atxdh1* Arabidopsis mutant. *The Plant Journal*, **54**, 496–509. Available from: https://doi.org/10.1111/j.1365-313X.2008.03440.x

Brychkova, G., **Xia, Z.**, **Yang, G.**, **Yesbergenova, Z.**, **Zhang, Z.**, **Davydov, O.** ***et al.*** (2007) Sulfite oxidase protects plants against sulfur dioxide toxicity. *The Plant Journal*, **50**, 696–709. Available from: https://doi.org/10.1111/j.1365-313X.2007.03080.x

Clough, S.J. & **Bent, A.F.** (1998) Floral dip: a simplified method for agrobacterium-mediated transformation of *Arabidopsis thaliana*. *The Plant Journal*., **6**, 735–743. Available from: https://doi.org/10.1046/j.1365-313x.1998.00343.x

González-Guzmán, M., **Abia, D.**, **Salinas, J.**, **Serrano, R.** & **Rodríguez, P.L.** (2004) Two new alleles of the *abscisic aldehyde oxidase 3* gene reveal its role in Abscisic acid biosynthesis in seeds. *Plant Physiology*, **135**, 325–333. Available from: https://doi.org/10.1104/pp.103.036590

Graan, T. & **Ort, D.R.** (1984) Quantitation of the rapid electron donors to P700, the functional plastoquinone pool, and the ratio of the photosystems in spinach chloroplasts. *The Journal of Biological Chemistry*, **22**, 14003–14010. Available from: https://doi.org/10.1016/S0021-9258(18)89845-3

Havaux, M. & **Triantaphylides, C.** (2009) Singlet oxygen in plants: production, detoxification and signaling. *Trends in Plant Science*, **14**, 219–228. Available from: https://doi.org/10.1016/j.tplants.2009.01.008

Ibdah, M., **Chen, Y.T.**, **Wilkerson, C.G.** & **Pichersky, E.** (2009) An aldehyde oxidase in developing seeds of Arabidopsis converts benzaldehyde to benzoic acid. *Plant Physiology*, **150**, 416–423. Available from: https://doi.org/10.1104/pp.109.135848

Keren, N., **Berg, A.**, **Van Kan, P.J.**, **Levanon, H.** and **Ohad, I.** (1997) Mechanism of photosystem II photoinactivation and D1 protein degradation at low light: the role of back electron flow. *Proceedings of the National Academy of Sciences of the United States of America*, **94**(4), 1579-1584. https://doi.org/10.1073/pnas.94.4.1579

Knox, J.P. & **Dodge, A.D.** (1984) Photodynamic damage to plant leaf tissue by Rose Bengal. *Plant Science Letters*, **37**, 3–7. Available from: https://doi.org/10.1016/0304-4211(84)90194-9

Koiwai, H., **Nakaminami, K.**, **Seo, M.**, **Mitsuhashi, W.**, **Toyomasu, T.** & **Koshiba, T.** (2004) Tissue-specific localization of an abscisic acid, enzyme AAO3, in Arabidopsis. *Plant Physiology*, **134**, 1697–1707. Available from: https://doi.org/10.1104/pp.103.036970

Koshiba, T., **Saito, E.**, **Ono, N.**, **Yamamoto, N.** & **Sato, M.** (1996) Purification and properties of flavin- and molybdenum-containing aldehyde oxidase from coleoptiles of maize. *Plant Physiology*, **110**, 781–789. Available from: https://doi.org/10.1104/pp.110.3.781

Kurmanbayeva, A., **Bekturova, A.**, **Srivastava, S.**, **Soltabayeva, A.**, **Asatryan, A.**, **Ventura, Y.** ***et al.*** (2017) Higher novel L-Cys degradation activity results in lower organic-S and biomass in sarcocornia than the related Saltwort, Salicornia. *Plant Physiology*, **175**, 272–289. Available from: https://doi.org/10.1104/pp.17.00780

Laemmli, U.K. (1970) Cleavage of structural proteins during the assembly of the head of bacteriophage T4. *Nature*, **227**, 680–685.

Mano, J. & **Biswas, M.S.** (2018) Analysis of reactive carbonyl species generated under oxidative stress. *Methods in Molecular Biology*, **1742**, 117–124. Available from: https://doi.org/10.1007/978-1-4939-7668-3_11

Mano, J., **Kanameda, S.**, **Kuramitsu, R.**, **Matsuura, N.** & **Yamauchi, Y.** (2019) Detoxification of reactive carbonyl species by glutathione transferase tau isozymes. *Frontiers in Plant Science*, **10**, 1–7. Available from: https://doi.org/10.3389/fpls.2019.00487

Mano, J., **Nagata, M.**, **Okamura, S.**, **Shiraya, T.** & **Mitsui, T.** (2014) Identification of oxidatively modified proteins in salt-stressed Arabidopsis: a carbonyl-targeted proteomics approach. *Plant and Cell Physiology*, **55**, 1233–1244. Available from: https://doi.org/10.1093/pcp/pcu072

Mano, J., **Tokushige, K.**, **Mizoguchi, H.**, **Fujii, H.** & **Khorobrykh, S.** (2010) Accumulation of lipid peroxide-derived, toxic α,β-unsaturated aldehydes (E)-2-pentenal, acrolein and (E)-2-hexenal in leaves under photoinhibitory illumination. *Plant Biotechnology*, **27**, 193–197. Available from: https://doi.org/10.5511/plantbiotechnology.27.193

Mano, J., **Torii, Y.**, **Hayashi, S.**, **Takimoto, K.**, **Matsui, K.**, **Nakamura, K.** ***et al.*** (2002) The NADPH:Quinone oxidoreductase P1-ζ-crystallin in Arabidopsis catalyzes the α,β-hydrogenation of 2-alkenals: detoxication of the lipid peroxide-derived reactive aldehydes. *Plant and Cell Physiology*, **43**, 1445–1455. Available from: https://doi.org/10.1093/pcp/pcf187

Matsui, K., **Sugimoto, K.**, **Kakumyan, P.**, **Khorobrykh, S.** & **Mano, J.** (2009) Volatile oxylipins formed under stress in plants. *Methods in Molecular Biology*, **580**, 17–27. Available from: https://doi.org/10.1007/978-1-60761-325-1_2

Mendel, R.R. (2022) The history of the molybdenum cofactor—a personal view. *Molecules*, **27**, 4934. Available from: https://doi.org/10.3390/molecules27154934

Nurbekova, Z., **Srivastava, S.**, **Standing, D.**, **Kurmanbayeva, A.**, **Bekturova, A.**, **Soltabayeva, A.** ***et al.*** (2021) Arabidopsis aldehyde oxidase 3, known to oxidize abscisic aldehyde to abscisic acid, protects leaves from aldehyde toxicity. *The Plant Journal*, **108**, 1439–1455. Available from: https://doi.org/10.1111/tpj.15521

Oberschall, A., **Deák, M.**, **Török, K.**, **Sass, L.**, **Vass, I.**, **Kovács, I.** ***et al.*** (2000) A novel aldose/aldehyde reductase protects transgenic plants against lipid peroxidation under chemical and drought stresses. *The Plant Journal*, **24**, 437–446.

Omarov, R.T., **Akaba, S.**, **Koshiba, T.** & **Lips, S.H.** (1999) Aldehyde oxidase in roots, leaves and seeds of barley (*Hordeum vulgare* L.). *Journal of Experimental Botany*, **50**, 63–69. Available from: https://doi.org/10.1093/jxb/50.330.63

Omarov, R.T., **Sagi, M.** & **Lips, S.H.** (1998) Regulation of aldehyde oxidase and nitrate reductase in roots of barley (*Hordeum vulgare* L.) by nitrogen source and salinity. *Journal of Experimental Botany*, **49**, 897–902. Available from: https://doi.org/10.1093/jxb/49.322.897

Oshanova, D., **Kurmanbayeva, A.**, **Bekturova, A.**, **Soltabayeva, A.**, **Nurbekova, Z.**, **Standing, S.** ***et al.*** (2021) Level of sulfite oxidase activity affects sulfur and carbon metabolism in *Arabidopsis*. *Frontiers in Plant Science*, **12**, 690830. Available from: https://doi.org/10.3389/fpls.2021.690830

Rothe, G.M. (1974) Aldehyde oxidase isoenzymes (E.C.1.2.3.1) in potato tubers (*Solanum tuberosum*). *Plant and Cell Physiology*, **15**, 493–499. Available from: https://doi.org/10.1093/oxfordjournals.pcp.a075029

Ruggiero, B., **Koiwa, H.**, **Manabe, Y.**, **Quist, T.M.**, **Inan, G.**, **Saccardo, F.** ***et al.*** (2004) Uncoupling the effects of abscisic acid on plant growth and water relations. Analysis of sto1/nced3, an abscisic acid-deficient but salt stress-tolerant mutant in *Arabidopsis*. *Plant Physiology*, **136**, 3134–3147. Available from: https://doi.org/10.1104/pp.104.046169

Sagi, M., **Fluhr, R.** & **Lips, S.H.** (1999) Aldehyde oxidase and xanthine dehydrogenase in a flacca tomato mutant with deficient abscisic acid and wilty phenotype. *Plant Physiology*, **120**, 571–577. Available from: https://doi.org/10.1104/pp.120.2.571

Sagi, M., **Omarov, R.T.** & **Lips, S.H.** (1998) The Mo-hydroxylases xanthine dehydrogenase and aldehyde oxidase in ryegrass as affected by nitrogen and salinity. *Plant Science*, **135**, 125–135. Available from: https://doi.org/10.1016/S0168-9452(98)00075-2

Sagi, M., **Scazzocchio, C.** & **Fluhr, R.** (2002) The absence of molybdenum cofactor sulfuration is the primary cause of the flacca phenotype in tomato plants. *The Plant Journal*, **31**, 305–317. Available from: https://doi.org/10.1046/j.1365-313X.2002.01363.x

Seo, M., **Koiwai, H.**, **Akaba, S.**, **Komano, T.**, **Oritani, T.**, **Kamiya, Y.** ***et al.*** (2000) Abscisic aldehyde oxidase in leaves of *Arabidopsis thaliana*. *The Plant Journal*, **23**, 481–488.

Seo, M. & **Koshiba, T.** (2002) Complex regulation of ABA biosynthesis in plants. *Trends in Plant Science*, **7**, 41–48. Available from: https://doi.org/10.1016/S1360-1385(01)02187-2

Seo, M., **Peeters, A.J.M.**, **Koiwai, H.**, **Oritani, T.**, **Marion-Poll, A.**, **Zeevaart, J.A.D.** ***et al.*** (2000) The Arabidopsis aldehyde oxidase 3 (AAO3) gene product catalyzes the final step in abscisic acid biosynthesis in leaves. *Proceedings of the National Academy of Sciences*, **97**, 12908–12913. Available from: https://doi.org/10.1073/pnas.220426197

Soltabayeva, A., **Bekturova, A.**, **Kurmanbayeva, A.**, **Oshanova, D.**, **Nurbekova, Z.**, **Srivastava, S.** ***et al.*** (2022) Ureides are accumulated similarly in response to UV-C irradiation and wounding in Arabidopsis leaves but are remobilized differently during recovery. *Journal of Experimental Botany*, **73**(3), 1016–1032. Available from: https://doi.org/10.1093/jxb/erab441

Srivastava, S., **Brychkova, G.**, **Yarmolinsky, D.**, **Soltabayeva, A.**, **Samani, T.** & **Sagi, M.** (2017) Aldehyde oxidase 4 plays a critical role in delaying silique senescence by catalyzing aldehyde detoxification. *Plant Physiology*, **173**, 1977–1997. Available from: https://doi.org/10.1104/pp.16.01939

Stiti, N., **Adewale, I.O.**, **Petersen, J.**, **Bartels, D.** & **Kirch, H.H.** (2011) Engineering the nucleotide coenzyme specificity and sulfhydryl redox sensitivity of two stress-responsive aldehyde dehydrogenase isoenzymes of *Arabidopsis thaliana*. *Biochemistry Journal*, **434**, 459–471. Available from: https://doi.org/10.1042/BJ20101337

Sunkar, R., **Bartels, D.** & **Kirch, H.H.** (2003) Overexpression of a stress-inducible aldehyde dehydrogenase gene from *Arabidopsis thaliana* in transgenic plants improves stress tolerance. *The Plant Journal*, **35**, 452–464. Available from: https://doi.org/10.1046/j.1365-313X.2003.01819.x

Sussmilch, F.C., **Brodribb, T.J.** & **McAdam, A.M.S.** (2017) Up-regulation of NCED3 and ABA biosynthesis occur within minutes of a decrease in leaf turgor but AHK1 is not required. *Journal of Experimental Botany*, **68**, 2913–2918. Available from: https://doi.org/10.1093/jxb/erx124

Triantaphylides, C., **Krischke, M.**, **Hoeberichts, F.A.**, **Ksas, B.**, **Gresser, G.**, **Havaux, M.** ***et al.*** (2008) Singlet oxygen is the major reactive oxygen species involved in photooxidative damage to plants. *Plant Physiology*, **148**, 960–968. Available from: https://doi.org/10.1104/pp.108.125690

Tureckova, V., **Novak, O.** & **Strnad, M.** (2009) Talanta Profiling ABA metabolites in Nicotiana tabacum L. leaves by ultra-performance liquid chromatography – electrospray tandem mass spectrometry. *Talanta*, **80**, 390–399. Available from: https://doi.org/10.1016/j.talanta.2009.06.027

Widhalm, J.R. & **Dudareva, N.** (2015) A familiar ring to it: biosynthesis of plant benzoic acids. *Molecular Plant*, **8**, 83–97. Available from: https://doi.org/10.1016/j.molp.2014.12.001

Yamauchi, Y., **Furutera, A.**, **Seki, K.**, **Toyoda, Y.**, **Tanaka, K.** & **Sugimoto, Y.** (2008) Malondialdehyde generated from peroxidized linolenic acid causes protein modification in heat-stressed plants. *Plant Physiology and Biochemistry*, **46**, 786–793. Available from: https://doi.org/10.1016/j.plaphy.2008.04.018

Yamauchi, Y., **Hasegawa, A.**, **Taninaka, A.**, **Mizutani, M.** & **Sugimoto, Y.** (2011) NADPH-dependent reductases involved in the detoxification of reactive carbonyls in plants. *The Journal of Biological Chemistry*, **286**, 6999–7009. Available from: https://doi.org/10.1074/jbc.M110.202226

Yarmolinsky, D., **Brychkova, G.**, **Fluhr, R.** & **Sagi, M.** (2013) Sulfite reductase protects plants against sulfite toxicity. *Plant Physiology*, **161**, 725–743. Available from: https://doi.org/10.1104/pp.112.207712

Yergaliyev, T.M., **Nurbekova, Z.**, **Mukiyanova, G.**, **Akbassova, A.**, **Sutula, M.**, **Zhangazin, S.** ***et al.*** (2016) The involvement of ROS producing aldehyde oxidase in plant response to Tombusvirus infection. *Plant Physiology and Biochemistry*, **109**, 36–44. Available from: https://doi.org/10.1016/j.plaphy.2016.09.001

Yesbergenova, Z., **Yang, G.**, **Oron, E.**, **Soffer, D.**, **Fluhr, R.** & **Sagi, M.** (2005) The plant Mo-hydroxylases aldehyde oxidase and xanthine dehydrogenase have distinct reactive oxygen species signatures and are induced by drought and abscisic acid. *The Plant Journal*, **42**, 862–876. Available from: https://doi.org/10.1111/j.1365-313X.2005.02422.x

Yin, L., **Mano, J.**, **Wang, S.**, **Tsuji, W.** & **Tanaka, K.** (2010) The involvement of lipid peroxide-derived aldehydes in aluminum toxicity of Tobacco roots. *Plant Physiology*, **152**, 1406–1417.

Zdunek-Zastocka, E., **Omarov, R.T.**, **Koshiba, T.** & **Lips, H.S.** (2004) Activity and protein level of AO isoforms in pea plants (*Pisum sativum* L.) during vegetative development and in response to stress conditions. *Journal of Experimental Botany*, **55**, 1361–1369.

Zdunek-Zastocka, E. & **Sobczak, M.** (2013) Expression of *Pisum sativum* PsAO3 gene, which encodes an aldehyde oxidase utilizing abscisic aldehyde, is induced under progressively but not rapidly imposed drought stress. *Plant Physiology and Biochemistry*, **71**, 57–66.